Effects of temperature and drought on the light response of ecosystem CO2 exchange

C. Yi,[1] R. Li,[2] P.S. Bakwin,[3] D.M. Ricciuto,[1] J. W. Munger,[4] S. C. Wofsy,[4] K. Wilson,[5] T. P. Meyers[5]

[1] Department of Meteorology, the Pennsylvania State University, University Park, PA 16802, USA.
Chuixiang Yi (814-865-9617; cxyi@essc.psu.edu)
Kenneth J. Davis (814-863-8601; davis@essc.psu.edu)
Daniel M. Ricciuto (814-865-9617; ricciuto@essc.psu.edu)

[2] Department of Statistics, the Pennsylvania State University, University Park, PA 16802, USA.
Runze Li, (814-865-1555 rli@stat.psu.edu)

[3] NOAA Climate Monitoring and Diagnostics Laboratory, 325 Broadway, Boulder, CO 80305, USA.
Peter S. Bakwin (303-497-6773 peter.bakwin@noaa.gov)

[4]Department of Earth and Planetary Sciences, Harvard University, Cambridge, MA 02138, USA.
J. William Munger (617-495-5361 jwm@io.harvard.edu)
Steven C. Wofsy (617-495-4566 scw@io.harvard.edu)

[5]NOAA/ATDD, PO Box 2456, Oak Ridge, TN 37831, USA
Kell Wilson (423-576-2317 wilson@atdd.noaa.gov)
Tilden P. Meyers (423-576-2317 meyers@atdd.noaa.gov)

Correspondence: Chuixiang Yi
Department of Meteorology
The Pennsylvania State University
416 Walker Building
University Park, PA 16802
Phone: (814) 865-9617
Fax: (814) 865-3663
Email: cxyi@essc.psu.edu

Abstract: Temperature and drought are expected to affect the response of net ecosystem-atmosphere exchange of CO_2 (F) to the photosynthetically active radiation (Q). We investigate this hypothesis by using statistical methods to analyze the multi-year growing season daytime data of F and climate variables measured by micrometeorological methods from four AmeriFlux sites (two deciduous forest sites, a mixed forest site, and a grassland site). Temperature has a strong impact on F at high Q for all the sites. At low Q, temperature effects for the deciduous forests are less important, but are significant for the grassland and mixed forest. A rectangular hyperbolic response function has been fitted as a varying-coefficient model for each site through the multi-year growing season data sets. The dependencies of the light response parameters (respiration, quantum yield and light-saturated photosynthetic capacity) on temperature are pronounced, especially at higher temperatures but the function is site-dependent. Drought reduces the ecosystem photosynthetic capacity significantly. Grassland ecosystems are more sensitive to drought than forest ecosystems. Robust diurnally asymmetric patterns of F with climate variables were found, and the physiological and physical reasons for the asymmetry are analyzed. The ecosystem equivalent conductance is universally much higher early in the morning than in the afternoon across all four sites, while the differences between mean ambient and intercellular CO_2 concentration are universally lower early in the morning than in the afternoon. The ecosystem water use efficiency is highest early in the morning, is sharply reduced through midmorning, and reaches minimum values around mid-afternoon when temperature and vapor pressure deficit are at a maximum. Our results suggest that temperature and drought affect the ecosystem light response curve substantially, but the mechanisms are not fully understood. It is very important to correctly incorporate the effects of temperature and drought on ecosystem light response into biochemical models for global change studies.

1. Introduction

Climate variables such as growing season temperature and moisture availability exert strong control over the net ecosystem exchange of CO_2 (F). Changes in growing season climate can shift the annual net carbon balance of a forest by roughly 2 tC ha^{-1} yr^{-1} [*Goulden et al*., 1996; *Barford et al*., 2001]. To better understand which climate factors control the terrestrial carbon sink/source and how they control it, we focus on daytime in the growing season to examine the relationships between F and climate variables based on the micrometeorological measurements from AmeriFlux [*Baldocchi et al*., 2001].

A fundamental relationship between F and climate variables is the response of CO_2 flux between a leaf and the atmosphere to the photosynthetically active radiation (Q), for example, which can be described by a rectangle hyperbolic function

$$F = R - \frac{a Q F_\infty}{a Q + F_\infty}, \qquad (1)$$

where R is the dark respiration rate (defined as the intercept on the y axis of a plot of F vs. Q), $F_¥$ is the light-saturated net photosynthetic rate, α is the apparent quantum yield ($\alpha = dF/dQ|_{Q=0}$). The F-Q relationship has been applied widely to canopy levels to assess

net primary productivity (NPP) since remote sensing data became available [e.g., *Montheith*, 1972; *McCree*, 1974; *Monteith*, 1977; *Ruimy et al*., 1996; *Ruimy et al*., 1999]. The light use efficiency (ε), which is the ratio of dry matter production to the absorbed light, is an important parameter in the production efficiency models. ε is the slope of the light response curve (1), its maximum is equal to the apparent quantum yield α and decreases to zero at light saturation [Prince, 1991]. The variation in ε is related to vegetation type and environmental stresses [*Jarvis and Leverenz*, 1983; *Prince*, 1991]. *Goetz and Prince* [1999] pointed out that there are significant uncertainties in determining ε values owing to a paucity of comparable measured values. Most estimates of ε are based on measurements of above ground components of the overstory layer, and do not include either below ground production and understory or ground cover vegetation, nor do they allow for the effects of decomposition and other carbon losses [*Gower et al*., 1999; *Geotz and Prince*, 1999]. The ecosystem is a nonlinear system in which the individual components are both competing and cooperating for the available resources and in stress responses [*Field*, 1991; *Goetz and Prince*, 1999]. The eddy covariance method provides a direct measurement of CO_2, water vapor and heat flux above the canopy. These eddy covariance measurements represent the net exchange between the whole ecosystem and the atmosphere. A number of studies have used eddy covariance measurements to study the *F*-*Q* relationship at the ecosystem scale [*Wofsy et al*., 1993; *Hollinger et al*., 1994; *Ruimy et al*., 1995; *Chen et al*., 1999; *Gu et al*., 2002; *Schmid et al*., 2000; *Flanagan et al*., 2002]. However, previous studies have treated the light response parameters (*R*, α and $F_{¥}$) as constants. These parameters, which describe the resource use efficiency of an ecosystem, are not constant and depend on nutrient availability, ambient CO_2 and climate conditions (e.g., temperature and moisture availability) [*Field and Mooney*, 1986; *Gutschick*, 1987; *Field*, 1991; *Lambers et al*., 1998; *Curtis and Wang*, 1998; *Carey et al*., 1998; *Curtis et al*., 2000].

Our goal in this paper is to study physiological processes at the ecosystem scale in order to enable greater realism in parameterizations for ecosystem modeling studies. The objectives of this paper are to examine: (1) the relationships between the light response parameters and temperature, (2) the effects of drought on the ecosystem photosynthetic capacity across four Ameriflux tower sites, (3) the differences in physiological functions (such as conductance and water use efficiency) at the ecosystem scale between morning and afternoon. The vapor pressure deficit (*VPD*) also has an important impact on the light response parameters. However, since *VPD* is highly correlated to temperature, either temperature or *VPD* is an independent variable of the light response parameters. *Yu et al*. [1996] found very different responses of stomatal opening of maize leaves to *VPD* in the afternoon from in the morning. We use the eddy covariance measurements to examine these diurnal asymmetric phenomena on an ecosystem scale.

2. Sites and Measurements

This study was carried out at four AmeriFlux sites: a 447-m-tall WLEF television transmitter tower in northern Wisconsin (45.95^{o}N, 90.27^{o}W, hereinafter referred to as WL); the Walker Branch Watershed Site in eastern Tennessee (35.96 ^{o}N, 84.29 ^{o}W, WB); the Harvard Forest Environmental Measurement Site in central Massachusetts (42.52^{o}N,

72.18°W, HV); and the Little Washita Watershed in southwest Oklahoma (34.96 °N, 97.98 °W, LW).

The WL site is in a region of cold temperate mixed forest with abundant wetlands. The dominant forest types are mixed northern hardwoods, aspen, pine, and forested wetlands. The topography is slightly rolling with an elevation difference of 45 m between the highest and the lowest elevations. The elevation changes create a heterogeneous landscape of saturated (wetland) and unsaturated (upland) soils. The uplands comprise about 63% of the area, and wetlands about 37% of the area [*Ahl et al*., 2003]. More information about vegetation distribution, soil characteristics, and logging history can be found in [*Bakwin et al*., 1998; *Mackay et al*., 2002; *Davis et al*., 2003].

The WB site is located in the southern section of the temperate deciduous forest biome in the eastern United States. The predominant species in the forest stand include oak, maple, tulip poplar and loblolly pine [*Wilson and Baldocchi*, 2001]. The forest has been growing since agricultural abandonment in1940. The site is in hilly terrain, and the upwind fetch of forest extends several kilometers in all directions [*Baldocchi et al*., 2000]. Detailed description of canopy structures, species composition, and soil characteristics is provided by [*Hutchison and Baldocchi*, 1989; *Johnson and van Hook*, 1989; *Wilson and Baldocchi*, 2000].

The HV site is located in a temperate hardwood forest that includes mixed hardwood and conifer forests, ponds, extensive spruce and maple swamps, and diverse plantations. The trees are 50~70 years old, dominated by red oak and red maple. The site is centered in a small level drainage, with a stream running from the north-west to the east within 50 m of the tower, and with a gentle upward slope for several hundred meters to the south-west [*Wofsy et al*., 1993; *Goulden et al*., 1996]. A considerable fetch area of the tower is poorly drained.

The LW site is in the southern part of the Great Plains of the United States. The 3 m tower is surrounded by a grazed pasture that is flat and provides a minimum fetch of 200 m in all sectors [*Meyers*, 2001]. Summers are typically long, hot and dry with an average daily high temperature in July of 34°C. The land cover is a mixture of grasses and weeds with a canopy height ranging from 30 to 60 cm. The predominant grass is a long-lived native bunchgrass often found with big bluestem grass, but is more drought resistant [*Meyers*, 2001].

The three-dimensional sonic anemometers on towers above the vegetation are used to measure the fluctuations of wind velocity and virtual temperature. The fluctuations of CO_2 and water vapor were measured by infrared absorption gas analyzers. Simultaneously, meteorological variables were measured by a set of micrometeorological instruments. These high frequency data were processed into half-hourly data sets so that the instrument response characteristics, their sampling rates and sampling duration were adequate for measuring CO_2 and energy fluxes above forests. The details of the measurement methods and accuracy analysis can be found in publications for each site: WL [*Bakwin et al*., 1998; *Berger et al.*, 2001; *Yi et al., 2000*; *Davis et al*., 2003]; WB

[*Baldocchi*, 1997; *Baldocchi et al*., 2000; *Wilson and Baldocchi*, 2000]; HV [*Wofsy et al*., 1993; *Goulden et al*., 1996]; LW [*Meyers*, 2001].

The data sets used in this study are daytime half-hourly data in the growing season (June through August), which were obtained from the FLUXNET database available at Oak Ridge National Laboratory's Data Archive Center. The data we used include the net ecosystem exchange of CO_2 (F), latent heat flux (E), photosynthetically active radiation (Q), air temperature (T), *VPD* and net radiation (R_n). The data are gap-filled and the filling methods are described in *Falge et al*. [2001a; 2001b]. The years of data for each site are as follows: WB (1995-1998); HV (1992-1999); WL (1997-1999); LW (1996-1998).

3. Methods

We hypothesize that *the light response parameters* (R, $F_{¥}$ and α) in (1) *are functions of temperature*. Thus, (1) is written as

$$F(T,Q) = R(T) - \frac{a(T)QF_{\infty}(T)}{a(T)Q + F_{\infty}(T)}, \tag{2}$$

or

$$F(T,Q) = f\{Q; b(T)\} + d, \tag{3}$$

where d is mean zero random error, and $f\{Q; b(T)\}$ is a nonlinear function of Q, and each component of $b(T)$ is a smoothing function of T. (2) or (3) is called a nonlinear varying coefficient model.

We use a nonparametric statistical method to estimate functions $b(T)$. One of the advantages of this statistical method is that it does not need to impose any assumption on function forms of $b(T)$. The Newton-Raphson algorithm was employed in searching for functions of $b(T)$. The details about the nonlinear varying coefficient model can be found in Appendix A and *Li et al*. [2003].

Two natural questions arising here are: (1) By using the nonlinear varying coefficient model, do we improve model fitting? (2) Do the unknown parameter functions $R(T)$, $\alpha(T)$ and $F_{¥}(T)$ really depend on T.

To answer the first question, residuals, R^2 and RMSE were computed for each data set of WB, HV, WL and LW. The definition of R^2 and RMSE are given below. Let $\hat{y}_i$ be the fitted value of y_i, where $y_{i's}$ are the observed value of F. As in the context of linear regression analysis, we will use R^2 and root mean squared error (RMSE) to assess how well an underlying model fits the data. In our analysis, R^2 and RMSE are defined as follows:

$$R^2 = 1 - \frac{\sum_{i=1}^{n} (y_i - \hat{y}_i)^2}{\sum_{i=1}^{n} (y_i - \bar{y}_i)^2},$$

where $\bar{y}$ is the sample of y_i, and

$$\text{RMSE} = \left\{ n^{-1} \sum_{i=1}^{n} (y_i - \hat{y}_i)^2 \right\}^{1/2}.$$

which are the same as those in the context of linear regression analysis. A higher value of R^2 means that the underlying model fits the data better. From the definitions, a smaller value of RMSE will result in a greater R^2.

To answer the second question, we need new statistical tools developed recently. This question can be formulated to be a statistical testing hypothesis:

$$H_0 : R(T) \equiv R_0,\ a(T) \equiv a_0, \text{ and } F_\infty(T) \equiv F_{\infty,0}$$

against H_1: H_0 is not true, where R_0, α_0 and $F_{\infty,0}$ are unknown constants not depending on T. Thus, under the null hypothesis H_0, model (3) reduces to model (1). The underlying statistical hypothesis is different from traditional ones because we are testing whether or not an unknown function is equal to a constant. This kind of statistical hypothesis is referred to as nonparametric goodness-of-fit test. The topic of nonparametric goodness-of-fit currently is a very active research area, and some new results have been published in very recent statistical literatures (e. g. *Hart*, 1997; *Cai et al*., 2000; *Fan et al*., 2001; *Fan and Li*; 2002). In what follows, we generalize the idea of likelihood ratio test [*Cai et al.*, 2000] to model (3).

To construct a generalized likelihood ratio test [*Fan et al*., 2001] for our statistical hypothesis, assume that the random error d in model (3) is normally distributed with zero mean and variance s^2, and assume that the collected are independent random sample from model (3). Denote by $\hat{y}_{i0}$ and $\hat{y}_{i1}$ to be the fitted value of y_i under H_0 and H_1, respectively. Furthermore,

$$\hat{s}_0^2 = \frac{1}{n} \sum_{i=1}^{n} (y_i - \hat{y}_{i0})^2$$

and

$$\hat{s}_1^2 = \frac{1}{n} \sum_{i=1}^{n} (y_i - \hat{y}_{i1})^2$$

are the mean squared error under H_0 and H_1, respectively. The logarithm of the generalized likelihood ratio test (*GLRT*) is

$$GLRT = \ell(H_0) - \ell(H_1) = \frac{n}{2}\log\left(\frac{\hat{s}_0^2}{\hat{s}_1^2}\right),$$

where n is the sample size, $\ell(H_0)$ and $\ell(H_1)$ stand for the logarithm of likelihood under H_0 and H_1, respectively. In very general statistical settings, *Fan et al*. [2001] showed that the null asymptotic distribution *GLRT* does not depend on the unknown parameters R_0, α_0 and $F_{¥,0}$, which is referred to as Wilk's phenomenon, and further $r_K GLRT$ is asymptotically distributed to a chi-square distribution, where r_K is a constant depending on the kernel density function, and r_K=2.5375 for the Gaussian kernel used in our implementation. *Cai et al*. [2000] suggested using a bootstrap technique to obtain the null distribution. Intuitively, we may use polynomials to fit the estimated coefficients. We may further increase the degree of polynomials such that the polynomial fits are almost perfect. Thus, the total number of parameters used in the polynomial fit can be regarded as the number of parameters used to fit model (3) under H_1. This provides us a simple way to approximate the degrees of freedom (d.f.) of the asymptotic chi-square distribution. Therefore, we can calculate the approximate P-value.

4. Results and Discussions

4.1 Model Test and Comparisons

The residual plots for the four sites are depicted in Figure 1, in which the nonlinear varying coefficient model improves the fitting when the value of *F* is far away from zero. The nonlinear varying coefficient model also improves R^2 and RMSE. This indicates that the nonlinear varying coefficient model is better than model (1).

The *GLRT*s and the P-values for the four sites are listed in Table 1, from which it can be seen that all P-values are less than 0.0001, the *GLRT* rejects the null hypothesis for all of the four sites. In other words, the parameter functions $R(T)$, $\alpha(T)$ and $F_{¥}(T)$ really depend on *T*. The mean values of these parameters are close to the previous estimations. However, the temperature dependence of these parameters sheds light on how an ecosystem responds to environmental stresses. This is discussed in following sections.

It is noteworthy that the extremely large fluxes (positive and negative) measured were insensitive to modeling methods (Figure 1). This may imply that these unusually large fluxes were caused not by biological activities and possibly by other factors, such as weather system events, atmospheric turbulence events and errors in the eddy covariance technique. *Hurwitz et al*. [2002] reported that deep tropospheric mixing caused CO_2 mixing ratios to change rapidly, for example, in one summer convective event, CO_2 mixing ratios rose more than 22 ppm in a 400-m layer in just 90 seconds.

4.2 Temperature effect

Figure 2 shows that temperature plays a very important role in the net uptake of CO_2 of an ecosystem in high light conditions. The range of the temperature optimum for CO_2 uptake at high light is different from site to site, depending upon the normal temperature to which the ecosystem is adapted [*Larcher*, 1980]. For the sites WB and LW at lower latitude (about 35°N), the temperature optima are around 25 °C, for the other sites HV (43°N) and WL (46°N) the optima range about 10~17 °C. However, the optimal range of temperature does not coincide with the range of the most probable temperatures (Figure 3d). Most of the optimal temperatures are lower than the most probable temperatures, as is seen by comparing Figure 2 with Figure 3d. This implies that at high light conditions, net uptake of CO_2 is temperature-limited. For the HV and LW sites, the net uptake of CO_2 falls off sharply with high temperatures because at high temperatures, the oxygenating reaction of Rubisco increases more than the carboxylating one so that photorespiration becomes proportionally more important [*Lambers et al*, 1999; *Long*, 1991]. Heterotrophic respiration also increases with increasing temperature. The optimum range of temperature in grassland ecosystem seems to be narrower than in forest ecosystems. There is some indication that the optimum temperature for net uptake of CO_2 decreases with decreasing light intensity (Figure 2a and c). It is evident that an ecosystem has the ability to adapt to environmental stresses, i. e. optimum temperature is lower under low light conditions, implying the functional convergence hypothesis proposed by *Field* (1991). At low light, the temperature effects on F are very weak at WB and HV sites (Figure 2a-b), but significant at WL and LW sites (Figure 2c-d).

The light response parameters obtained by fitting the varying-coefficient model (2) with flux tower data are whole ecosystem parameters. For example, "dark respiration" R can be regarded as ecosystem respiration rate that includes leaf, stem and root respiration and soil organic matter decomposition [*Hanan et al*., 2002; *Kelly et al*., 2002; *Gu et al*., 2002]. The temperature dependencies of the light response parameters are pronounced, as shown in Figure 3. On average, the magnitudes of these parameters are consistent with those estimated by *Ruimy et al*. [1995]. The ecosystem respiration rates for the deciduous forest sites HV and WB are linear increasing functions of temperature (Figure 3a). For the grassland site LW, the ecosystem respiration is lowest amongst the four sites as the temperature is lower, but it increases rapidly with increasing temperature, and saturates when temperature is higher than 25 °C. The WL site has an optimal range of temperature for ecosystem respiration that coincides with the most probable temperature (Figure 3a,d).

The light-saturated net photosynthetic rate $F_{¥}$ is a gross assimilation rate at saturating Q, which is limited by a number of factors that include both biochemical (e.g. leaf nitrogen content, CO_2) and non-biochemical factors (e.g. temperature, *VPD*, soil water). The effects of biochemical factors on $F_{¥}$ are ignored in this paper. We take temperature effects into consideration but neglected the relationship between leaf nitrogen content and temperature, which we assume to be weak. However, we cannot rule out the water stress effect from the relationship between $F_{¥}$ and temperature because high temperature often coincides with drought [*Lambers et al*., 1998]. Figure 3b shows that $F_{¥}$ is significantly affected by temperature. The way that $F_{¥}$ is regulated by temperature is different amongst the four sites. $F_{¥}$ of the mixed forest ecosystem (WL) decreases linearly with increasing

temperature at a rate of about 0.9 μmol m^{-2} s^{-1} $^oC^{-1}$ (Figure 3d). For WB site, $F_¥$ slowly decreases with increasing temperature at a rate of about 0.53 μmol m^{-2} s^{-1} $^oC^{-1}$ when temperature is lower than 28^{o}C and then decreases dramatically with increasing temperature at a rate of about 5.0 μmol m^{-2} s^{-1} $^oC^{-1}$. The temperatures that dramatically reduce $F_¥$ are the most probable afternoon temperatures. Therefore, the dramatic drop of $F_¥$ may result from water stress with higher *VPD* (Figure 4b or Figure 9b). For the grassland ecosystem LW, there is an optimal temperature of $F_¥$ that is close to the most probable temperature (Figure 3b,d). This kind of $F_¥$ -*T* relationship is typical in the predictions by a physiological mechanistic model of leaf photosynthesis [*Farquhar et al*., 1980; *Farquhar & von Caemmerer*, 1982; *Long*, 1985; *Long*, 1991]. Why is the $F_¥$ -*T* relationship of grassland ecosystem close to the leaf model prediction and not for the forest ecosystem? The grassland ecosystem has simpler vertical canopy structure relative to the forest ecosystems and is more uniform in horizontal and root depth, i.e. more close to the "big leaf" assumption. Forest ecosystems are much more complicated. For example, while the overstory is light saturated, the understory is still light limited, and water stress on the overstory may result from the deep soil water availability while water stress on the understory may result from shallow soil water availability [*Lee*, 1980]. The physiological explanation for the $F_¥$ -*T* relationship of grassland ecosystem could be given as follows: below the optimal temperature, ecosystem respiration is temperature limited (Figure 3a,b); beyond the optimal temperature, the ratio of carboxylation rates to oxygenation rates decrease as temperature increases [*Long*, 1991]. For the forest ecosystem at HV, the temperature response of $F_¥$ was substantially different from the other sites. $F_¥$ was lower under low temperature and increased with increasing temperature at a rate of about 1.3 μmol m^{-2} s^{-1} $^oC^{-1}$ and saturated beyond the most probable temperature of around 23 ^{o}C. The reason that no reduction in $F_¥$ at high temperature occurs may be that water stress is not critical for the HV site [*Yi et al*., 2003a]. This will be discussed further in Section 4.4.

The apparent quantum yield α represents the maximum light use efficiency of an ecosystem. It varies with vegetation type as shown in Figure 3c. The average values of α were 0.051 at HV, 0.040 at WB, 0.028 at WL and 0.019 at LW. The light use efficiencies for the deciduous forest ecosystems (HV and WB) were highest, and α was lowest for the grassland ecosystem LW, which was dominated by C3 plants. The mixed forest ecosystem WL has a relatively low light use efficiency possibly because the light use efficiency in wetlands is lower. The hardwood ecosystem α (0.051) is higher than the broadleaf forest ecosystem α (0.037, *Ruimy et al*. [1995]) and close to a boreal aspen forest ecosystem (0.045 and 0.052, *Chen et al.*, [1999]). The α values of the deciduous forest ecosystem (0.040), the mixed forest ecosystem (0.028) and grasslands ecosystem (0.019) are close to the α values of the broadleaf forest ecosystem (0.037), conifer forest ecosystem (0.024), and C3 grasslands ecosystem (0.017) estimated by *Ruimy et al*. [1995], respectively.

The temperature sensitivity of α was significant within some temperature ranges. For the WB site, α is almost constant as the temperature is below 19 ^{o}C, and then decreases rapidly with increasing temperature from 0.044 to 0.031 at a temperature of about 32 ^{o}C.

At temperatures higher than 32 ^{o}C, α becomes invariably lower. The most sensitive temperatures at WB were the most probable and high temperatures (Figure 3c,d). Therefore, statistically, α of the deciduous forest ecosystem at WB is temperature dependent. The mixed forest ecosystem (WL) α is also temperature dependent, with quite low values at low temperatures increasing slowly with increasing temperature and saturating at about 29 ^{o}C. The hardwood forest ecosystem (HV) α increases rapidly with increasing temperature at the low temperature, but this is statistically meaningless because the probability densities of occurrence of these temperatures are close to zero (Figure 3d). At temperatures higher than 13 ^{o}C, α slightly decreases with increasing temperature, and hence the temperature sensitivity of α at HV is weak. The grassland ecosystem (LW) α appears to be statistically insensitive to changes in temperature at temperatures lower than the most probable temperature of around 30 ^{o}C. However, at temperatures higher than 30 ^{o}C, increasing temperature extremely enhances α, which attains a value of about 0.038 at about 37 ^{o}C (Figure 3c). The higher α values appearing at higher temperatures (Figure 3c) are close to the α range from 0.021 to 0.051 *Suyker and Verma* [2001] found for C4 grasslands ecosystem. C4 grassland ecosystems usually have higher values of α than C3 grassland ecosystems [*Ruimy et al*., 1995]. C4 plants have fewer stomata than C3 plants, resulting in decreased water loss so that C4 plants do better in hotter and drier conditions. The seasonality of α for C4 grassland ecosystems, found by *Gu et al*.[2002], is such that α values at mid-summer are much higher than in spring and autumn. This might imply that α for C4 grassland ecosystems would increase with increasing temperature. Even if this is true, we would still have difficulty explaining the behavior of the grassland ecosystem α at higher temperatures because C4 species of the grassland ecosystem at LW are only one third of the total. Also, C3 plant α decreases physiologically with increasing temperature due to the proportionally increasing oxygenating activity of Rubisco [*Lambers*, 1999].

4.3 Diurnal Asymmetry

In this section we examine how climate factors control the net ecosystem exchange of CO_2 and H_2O in the course of daytime by using the ensemble average method. Statistically, the ecosystems (WB, WL and LW) have more net uptake of CO_2 in the morning than in the afternoon while HV ecosystem has a close symmetric distribution of net uptake of CO_2 around noon. This asymmetric distribution of net uptake of CO_2 around noon is typical [*Price and Black*, 1990; *Jarvis et al*., 1997; *McCaughey et al*., 1997; *Hollinger et al*., 1998; *Pilegaard et al*., 2001; *Flanagan et al*., 2002]. The effect of morning advection on measured *F* [*Yi et al*., 2000], essentially a measurement bias, may be one cause for the asymmetry. However, the most important reason may be that physiological responses of an ecosystem to environmental stress in the afternoon are different from in the morning [*Meidner and Mansfield*, 1968; *Lambers et al*., 1998]. Climate variables *Q*, R_n, *T* and *VPD* coincidentally increase in the morning; however, *Q* and R_n have symmetric distributions around noon, statistically, and *T* and *VPD* reach their maximum values about 2~3 hours later (Figure 4, Figure 5). Net uptake of CO_2 increases with increasing *T* (or *VPD*) and *Q* (or R_n), reaches maximum values by about 10:30 a.m., and remains relatively constant with time as *T* (or *VPD*) reaches a maximum. The time when *T* (or *VPD*) reaches a maximum value is a turning point after which net uptake of

CO_2 decreases rapidly with decreasing temperature (or *VPD*) (Figure 4a,b and Figure 5a,b). At the same values of *Q*, the net uptake of CO_2 in the afternoon is significantly less than that in the morning (Figure 4c,d and Figure 5c,d). This nonlinear hysteresis phenomenon may reflect temperature (or *VPD*) effects on stomatal openings. A frequently observed pattern of behavior in plants growing in hot climates is wide stomatal openings in the morning, partial or even complete closure sometime after midday, followed by reopening in the afternoon [*Meidner and Mansfield*, 1968]. Stomatal openings are also sensitive to water stress. Plants take water from roots and lose water from leaves. Sap-flow measurements demonstrate that the time lag between transpiration and tree root water uptake is as much as 3 hours [*Moren et al*., 2000]. No soil water data were available to examine how the time lag induces the hysteresis phenomenon. However, it is clear that the second turning point was related to maximum environmental stress in a day, such as *T* and *VPD* were maximum at the turning point.

While net uptake of CO_2 saturates at about 10:30 a.m. (Figure 4b, 5b), the evapotranspiration *E* still increases with increasing *VPD* until sometime after midday (Figure 4f, 5f), indicating that the maximum net uptake of CO_2 does not coincide with the maximum evapotranspiration. Consequently, the ecosystem water use efficiency (WUE), defined as $|A|/E$, is lower in the afternoon than in the morning (Figure 4g and Figure 5g).

To determine which physiological mechanisms are responsible for the difference in WUE between morning and afternoon, we calculated the gross assimilation *A* by the light response model (2) based on data of *F*, *Q* and *T*. The relationship between *A* and *E*, as shown in Figure 6, is similar to the relationship between *F* and *E* (Figure 4f and Figure 5f). We assume that the leaf level relationships

$$A = g(c_a - c_i) = g\Delta c\,, \tag{4}$$

$$E = 1.6g(e_i - e_a) = 1.6gVPD\,, \tag{5}$$

can be applied to ecosystem level, where *A* is a gross assimilation rate, c_i and c_a are leaf intercellular and ambient carbon dioxide concentrations, respectively, e_i and e_a are the respective water vapor pressure, *g* is stomotal conductance, and 1.6 is the ratio of the diffusivities of water and carbon dioxide in air [*Infante et al*., 1999; *Yu et al*., 2001]. At the ecosystem level, *g* can be considered as an equivalent canopy conductance, c_i and e_i the mean canopy intercellular CO_2 concentration and water vapor pressure, respectively. The generalization of (5) from a leaf to an ecosystem seems to be rough, however, it is at least plausible for the assumption that evapotranspiration is proportional to *gVPD* [*Jarvis and McNaughton*, 1986; *Nemani and Running*, 1989]. Applying (4) and (5) to the following equation

$$E_{am}(g_{am}, VPD_{am}) = E_{pm}(g_{pm}, VPD_{pm})$$

defined in Figure 6, where subscript am and pm indicate morning and afternoon, respectively, we obtained

$$\frac{g_{am}}{g_{pm}} = \frac{VPD_{pm}}{VPD_{am}}, \tag{6}$$

$$\frac{\Delta c_{am}}{\Delta c_{pm}} = \frac{g_{pm}}{g_{am}} \frac{A_{am}}{A_{pm}}. \tag{7}$$

The variables on the right-hand side of (6) and (7) are measured. Thus, the ratios of g_{am}/g_{pm}, $\Delta c_{am}/\Delta c_{pm}$ are estimated. As shown in Figure 7, as midday approaches, the ratios $\Delta c_{am}/\Delta c_{pm}$ increased towards one, while the ratios g_{am}/g_{pm} strongly decline towards one. This pattern was quite universal across the four sites. The equivalent canopy conductance was four or five times higher early in the morning than in late afternoon, noting that the definition of morning and the conjugate afternoon was constrained by the same amount of evapotranspiration as shown in Figure 6. A number of field measurements show similar asymmetric distributions for leaf conductance [*Pallardy and Kozlowski*, 1981; *Schulze and Hall*, 1982; *Jurik et al*., 1985; *Sala and Tenhunen*, 1994; *Sala and Tenhunen*, 1996; *Yu et al*., 1996a; *Infante et al*., 1999]. Whether at leaf level or at ecosystem level, it is very common that morning conductance is higher than afternoon conductance. This very asymmetric distribution appears to be a result of the responses of stomatal aperture to *VPD* (or temperature), which is a drought avoidance response of an ecosystem to conditions conducive to water deficits.

The conductance ratio g_{am}/g_{pm} is inversely correlated to the CO_2 gradient ratio $\Delta c_{am}/\Delta c_{pm}$ (Figure 7). The decreases in the CO_2 gradient ratio $\Delta c_{am}/\Delta c_{pm}$ with time imply that the mean canopy intercellular CO_2 concentration c_i is higher in the morning than in the afternoon for a given amount of evapostranspiration. c_i is determined by the balance between photosynthetic removal and respiratory production of CO_2 inside the leaf, and may change from several thousand ppm in darkness with closed stomata to less than 200 ppm at light-saturated. The value of c_i in C3 plants during light-saturated photosynthesis is usually in the range 180-230 ppm [*Jarvis and Sandford*, 1986]. The gross assimilation rates *A*, conductance *g* and intercellular CO_2 concentration c_i are closely linked to each other, as shown schematically in Figure 8. The supply function describes the process of diffusion, and is shown as a dashed line with a negative slope. The magnitude of the slope is equal to the stomatal conductance. In general, if c_i decreases as *A* decreases, then *A* is "supply-limited", which implies that stomatal closure caused the decrease. Ambient CO_2 concentration c_a is high early in the morning due to the respiratory release of CO_2 accumulated in nocturnal boundary layer [*Yi et al*., 2001], and c_a gradually decreases to invariably lower values in afternoon due to a deeply developed convective boundary layer and photosynthesis [*Yi et al*., 2003b]. For example, in the growing season at the WL site, c_a at 7:30 a.m. was averaged about 385 ppm and remained almost constant at about 355 ppm for the whole afternoon. Therefore, early in the morning, the higher ambient CO_2 concentration c_a^{am} and higher conductance g_{am} (stomatal aperture wide opening) provided a "satisfied" supply conditions, leading to a higher c_i^{am} and A_{am} (Figure 8), noting that the actual A_{am} early in the morning was lower than the one shown in Figure 8 because of light-limited conditions. With increased *Q*, *T* and *VPD*, the light limitation on

assimilation rates becomes weaker but evaporative demand becomes stronger so that reductions in stomatal aperture are considerable in the afternoon. This results in a limited supply condition that leads to a lower c_i^{pm} and A_{pm} (Figure 8). It should be noted that while c_i depends on g, stomatal openings are also sensitive to c_i. The factors controlling stomatal opening are very complicated and some mechanisms are still unknown [*Meidner and Mansfield*, 1968; *Larcher*, 1980; *Lambers et al*., 1998].

Figure 9a shows the relationships between the ecosystem WUE and temperature across the four sites. The general diurnal pattern of WUE across the four sites is characterized by maximum values early in the morning, a sharp decrease through midmorning, a gradual decrease in early afternoon, and minimum values that are reached around mid-afternoon as temperature and *VPD* are maximum (Figure 9a,b). At the two high latitudinal sites (HV and WL) WUE is almost constant in the afternoon as compared to the morning. Higher WUE in the morning than in the afternoon has also been observed at the leaf level [*Infante et al*., 1999; *Zine El Abidine et al*., 1995]. This asymmetric pattern can be explained by the combination of relation (4) and (5): WUE is inversely proportional to *VPD*, as shown in Figure 9. *VPD* as a dominant factor controlling WUE is also supported by sap flux measurements [*Moren et al*., 2001; *Ewers et al*., 2002; *Mackay et al*., 2002]. *Ewers et al*. [2002] reported that transpiration of WL forest is highly correlated to *VPD* but not to soil moisture. The diurnally asymmetric distribution of WUE is similar to that of g and c_i due to WUE being mechanistically related to g and c_i. Figure 9a also indicates that the WUE of the grassland ecosystem is apparently lower than forest ecosystems.

4.4 Effect of Drought

In order to illustrate the effect of drought on F we superimposed the diurnal patterns of F with climate variables in a drought year (shown by red) and in a wet year (shown by blue) on Figure 4 and Figure 5. The drought (or wet) year was defined as a year that was relative drier (or wetter) among the data available years for each site based on annual precipitation and net radiation data (Table 2). If the ecosystem photosynthetic capacity is defined as F_m, being F at maximum Q, the F_m was significantly reduced in the drought year and increased in wet year (Figure 4 and Figure 5). This drought effect is consistent across the four sites (WL and HV sites are not shown). In comparison with forest ecosystem, grassland ecosystem is more sensitive to drought. In the driest year 1998, the grassland ecosystem acted as a carbon source and there was not much photosynthetic activity (Figure 5). In the study of light response of F by the nonlinear varying-coefficient model (2) for LW, the data in 1998 are excluded because we could not obtain a convergent result. This also indicates that the main part of F in 1998 was the respiration component (see Figure 9 of *Meyers* [2001]). Although drought caused reduction in photosynthesis, respiration and evapotranspiration, photosynthesis may be the most sensitive to water stress. For example, while the photosynthesis of the grassland was almost completely inhibited in the driest year 1998 (Figure 5a,b), the maximum evapotranspiration in 1998 was just reduced to about half of that in the wettest year 1996 (Figure 5f). This led to lower WUE in drought conditions (not shown). When plants are subjected to water stress, the stomata tend to close. This closure response causes the decline in stomatal conductance and leads to the reduced slope of the supply function

with drought (Figure 8). Water stress reduces the ecosystem photosynthetic capacity F_m significantly, as illustrated in Figures 3 and 4.

F_m can be represented by mean F at noon over the growing season. We hypothesize that F_m is regulated by a radiative index of dryness [*Budyko*, 1974], which is defined as

$$I = \frac{\overline{R}_n}{L\overline{P}}, \tag{10}$$

where $\overline{R}_n$ (MJ m^{-2} yr^{-1}) is an annual sum of net radiation, L (2.5 MJ kg^{-1}) is a latent heat coefficient and $\overline{P}$ (mm yr^{-1}) is the total annual precipitation. Why is F_m in growing season related to the annual water supply? Because the water availability in the growing season is not only dependent on precipitation in the growing season but is also dependent on the water stored in cold seasons [*Meyers*, 2001, *Yi et al*., 2003b]. A good correlation between F_m and dryness was found across the four sites (Figure 10). Some differences of F_m in response to dryness from site to site existed (Figure 10). F_m is more sensitive to dryness at WB and LW, less sensitive at WL and insensitive at HV. The insensitivity of F_m to dryness at HV and lack of limitation of high temperature on $F_¥$ (Figure 3b) provide further evidence that water stress is not critical for HV. Soil water availability not only depends on precipitation but also is related to local topographic features, drainage conditions and ground water supply [*Lee*, 1980].

5. Concluding Remarks

The light response curve of a leaf for uptake of CO_2 is a fundamental function for modeling the terrestrial carbon sources/sinks, and a basic link for understanding the mechanisms of interaction between the atmosphere and ecosystems. Eddy covariance measurements allow scientists to examine the bulk properties of the light response parameters for ecosystems as a whole. These parameters have been treated previously as constants. We used a nonparametric statistical method to develop a nonlinear varying coefficient model and examined the relationships between the light response parameters and temperature. When the model was tested against the eddy covariance data and compared with the constant coefficient mode, the accuracy improved. The mean values of light response parameters obtained from the nonlinear varying coefficient model were close to those obtained by the others [*Ruimy et al*., 1995; *Suyker and Verma*, 2001]. However, the relationships between ecosystem light response parameters and temperature gives insight into how whole ecosystems respond to environmental stresses. Remarks on these relationships are as follows:

(1) *Ecosystem respiration R*. The overall trend was that *R* increased with increasing temperature, which was not surprising. However, the functional form of *R* with temperature were different from the exponential form as shown by nighttime fluxes versus temperature [e. g. *Black et al*., 1996; *Goulden et al*., 1997; *Lindroth et al*., 1998; *Pilegaard et al*., 2001; *Yi et al*., 2003a]. The biggest contrast was that daytime respiration at higher temperature was either temperature-limited or did not increase with temperature as strongly as expected in exponential form. There

are three reasons that daytime respiration is limited at higher temperature: (1) water stress on autotrophic respiration through stomatal closing; (2) water stress on heterotrophic respiration (strong evidence in *Borken et al.* [1999]); (3) temperature sensitivity of respiration is reduced at higher temperature [*Luo et al*., 2001; *Yi et al*., 2003a] due to daytime temperatures are higher than nighttime temperatures. Therefore, it is noteworthy that applying the regression relationship between nighttime CO_2 flux and temperature to model daytime respiration from daytime temperature observations may lead to a high bias at high temperature. In addition, our measurements were conducted under natural conditions and soil moisture might not be optimal. Reichstein et al [2002] reported that the apparent temperature sensitivity of ecosystem respiration declines with drought. Thus, the decline behavior of R at high temperature in Figure 3a may be also related to the drought effects.

(2) *Ecosystem light-saturated net photosynthetic rate* $F_{¥}$. Temperature effects on $F_{¥}$ were strong and site-dependent. The mechanisms for the $F_{¥}$–T relationships are poorly understood. The sharp fall-off in $F_{¥}$ for the ecosystems at WB and LW at higher temperature may result from higher *VPD* and stomata closure. The reason why increasing temperature caused an increase in $F_{¥}$ at HV and a reduction in $F_{¥}$ at WL are not clear. We hypothesize that this difference resulted from different water stress for the two ecosystems because the temperature effect may be confounded with a drought effect.

(3) *Ecosystem apparent quantum yield* α. α is dependent on vegetation type, and is highest for the deciduous forest ecosystems, lowest for the grassland ecosystem and intermediate for the mixed forest ecosystem. The effects of temperature on α are weak at HV, but very strong at high temperature for the other three sites. Increasing temperature enhances α greatly at high temperature for the grassland ecosystem at LW, which clearly contrasts with the results from a mechanistic model at the leaf level in which α in C3 species decreases with increasing temperature [*Long*, 1991].

Drought caused a significant reduction in the photosynthetic capacity F_m, as was seen by comparing the diurnal patterns of F with climate variables between wetter years and drier years. The grassland ecosystem was the most sensitive to drought. In the driest year 1998, photosynthesis in the grassland ecosystem was almost completely inhibited, and the relationship between the net uptake of CO_2 and temperature was similar to the relationship between respiration and temperature. It was very difficult to quantify and to separate the drought effect from the temperature effect because water stress often occurs simultaneously with high light and high temperature and is not additive. We used mean values of F around noon in the growing season as F_m and dryness index I for each site-year to examine their relationship. The strong trend of down-regulation of photosynthetic capacity in response to dryness was found across different ecosystems and different years, but mechanisms behind this were not yet fully understood.

Diurnally asymmetric patterns between ecosystem net uptake of CO_2 and climate variables were robust across the four sites. Our results are consistent with the notion that stomatal opening is the main limiting factor for photosynthesis. The mechanisms behind

this strong hysteretic phenomenon are that the equivalent canopy conductance and the mean canopy intercellular CO_2 concentrations are higher in the morning than in the afternoon. Ambient CO_2 concentrations are also usually higher early in the morning due to accumulated respiratory CO_2 in the previous nocturnal boundary layer, and CO_2 was lower in the afternoon due to photosynthetic depletion and deep turbulent mixing [*Yi et al.*, 2003b]. Under the same light-limited conditions, higher conductance, and intercellular and ambient CO_2 concentrations early in the morning led to the higher gross photosynthesis than in the afternoon. Similar to the equivalent canopy conductance, the ecosystem WUE was also diurnally asymmetric, being highest early in the morning and reaching a minimum value near the mid-afternoon when temperature and *VPD* are maximum. All of these diurnal asymmetric patterns mentioned above were linked with each other, and it is difficult to say which one was the cause or result. However, they all were the results of physiological responses of an ecosystem to environmental stresses. The time of day when temperature and *VPD* are maximum seems to be critical for the physiological responses of an ecosystem to environmental stresses. Photosynthetic carbon metabolism is an irreversible process. After passing through the critical point of maximum environmental stress, the function of photosynthetic response of an ecosystem cannot be recovered immediately. When comparing the relationship between *WUE* and *T* (Figure 9a) with the relationship between *VPD* and *T* (Figure 9b) around the critical point, it becomes clear that the physiological responses are different from physical responses. An ecosystem has the ability to adjust physiological function to adapt the environmental stresses [*Lambers et al*., 1998]. Physiological mechanisms around the critical point are yet unknown but crucial to understanding how an ecosystem responds to environmental stresses.

Appendix A: **Nonparametric Statistical Modeling**

A.1 Statistical Modeling

Regression is one of the most useful techniques in statistics. Let Y equal to F and $\mathbf{X}$ consist of Q and T. Of interest is to estimate the relationship between Y and $\mathbf{X}$ based on the collected sample $(\mathbf{x_1}, y_1), \ldots, (\mathbf{x_n}, y_n)$. A regression model may be used to describe this relationship:

$$Y = m(\mathbf{X}) + d,$$

where δ is a random error with zero mean, and $m(\mathbf{x})$ is the regression function, which characterizes the relationship between Y and $\mathbf{X}$. For a given data set, one may try to fit the data by using a linear regression model. In this paper, we are interested in nonlinear regression, such as model (1). To estimate parameters in nonlinear regression models, one needs to know the form of the nonlinear relationship. In practice, finding the nonlinear relationship may be a challenging task. Nonparametric regression models do not need to impose any assumption on functional form of the regression $m(\mathbf{x})$.

A.1 Kernel Estimator for $m(\mathbf{x})$

Usually, a datum point closer to **x** carries more information about the value of $m(\mathbf{x})$. Therefore an intuitive estimator for the regression function $m(\mathbf{x})$ is the running local average. An improved version of this is the locally weighted average. That is,

$$\hat{m}(\mathbf{x}) = \sum_{i=1}^{n} w_i(\mathbf{x}) Y_i / \sum_{i=1}^{n} w_i(\mathbf{x}),$$

where $w_i(\mathbf{x})$ are weights. An alternative interpretation of locally weighted average estimators is that the resulting estimator is the solution to the following weighted least-squares problem:

$$\min_q \sum_{i=1}^{n} (y_i - q)^2 w_i(\mathbf{x}).$$

A kernel estimation for $m(\mathbf{x})$ can be obtained by setting the weights $w_i(\mathbf{x}) = K_h(\mathbf{x}_i - \mathbf{x})$:

$$\hat{m}(x) = \frac{\sum_{i=1}^{n} K_h(\mathbf{x}_i - \mathbf{x}) y_i}{\sum_{i=1}^{n} K_h(\mathbf{x}_i - \mathbf{x})}, \qquad \text{(A1)}$$

where $K_h(.) = h^{-d} K(./h)$, d is the dimension of x, $K(.)$ is a kernel density function and h is called a bandwidth. In our implementation, the 2-dimensional Guassian kernel $K(\mathbf{x}) = (2p)^{-1} \exp(-\mathbf{x}^T \mathbf{x}/2)$ was used. There are a number of statistical papers that discuss how to obtain the bandwidth h [e. g. *Wand and Jones*, 1995]. The estimator $\hat{m}(\mathbf{x})$ can be used for visually exploring the relationship between Y and **X**. For instance, we may use the estimator to construct contour plots as shown in Figure 2.

A.2 Nonlinear Varying-Coefficient Model

One of objectives of this paper is to estimate the relationships between the light response parameters R, α and F_v in (2) and temperature. The nonparametric statistical method allows us to estimate these functions without assuming any functional forms for them. The nonlinear varying coefficient model (2) can be written as a general form

$$Y = f\{X_1; b(X_2)\} + d, \qquad \text{(A2)}$$

where d is mean zero random error, and $f\{X_1; b(X_2)\}$ is a nonlinear function of X_1, and each component of $b(x_2)$ is a smoothing function of x_2. Denote by d the dimension of $b(x_2)$.

Local linear regression techniques [*Fan and Gijbels*, 1996] are employed to construct an estimator for $b(x_2)$ and its derivatives. Using Taylor's expansion in a neighborhood of given x_{20}, for j = 1, …, d,

$$b_j(x_2) \approx b_j(x_{20}) + b_j(x_0)(x_2 - x_{20}) \equiv a_j + b_j(x_2 - x_{20}).$$

Denote $\mathbf{a} = (a_1, \ldots, a_d)^{\mathrm{T}}$ and $\mathbf{b} = (b_1, \ldots, b_d)^{\mathrm{T}}$. Thus, we obtain a local linear regression estimator $(\hat{a}^T, \hat{b}^T)^T$ by minimizing

$$l(\mathbf{a}, \mathbf{b}) = \frac{1}{2}\sum_{i=1}^{n}[y_i - f\{x_{1i}, \mathbf{a} + \mathbf{b}(x_{2i} - x_{20})\}]^2 K_h(x_{2i} - x_{20}). \qquad \text{(A3)}$$

That is, for j = 1, …, d, $\hat{b}_j(x_{20}) = \hat{a}_j$, and the first order derivatives of $\hat{b}(x_2)$ can be estimated via $\hat{b}_j'(x_{20}) = \hat{b}_j$. The details about the nonlinear varying coefficient models (A2) can be found in *Li et al*. [2002].

Note that the optimization problem in (A3) is indeed a nonlinear weighted least squares optimization. The Newton-Raphson algorithm was employed to search for a solution of (A3). The initial value for **a** in the Newton-Raphson algorithm is set to be the resulting estimate under model (1), and the initial value for **b** is set to be zero. In rare case, the ordinary Newton-Raphson algorithms with the given initial values fail to converge. In such a situation, the smaller step-length is set during the course of iterations. In our implementation, we found that this strategy works very well.

Let $x_{2,min}$ and $x_{2,max}$ be the minimum and maximum of $\{x_{2i}$, i=1,..., n$\}$, respectively. A *left boundary point* is thought of as being of the form $x_{20} = x_{2,min} + c\,h$, whereas a *right boundary point* x_{20} is of the form $x_{20} = x_{2,min} - c\,h$, where $0 \le c<1$. For the local linear regression estimator derived from (A3), the estimated coefficients at boundary points may have greater variation than that at points in the interior, referred as *boundary effects* or *edge effects* [*Fan and Gijbels*, 1996]. These effects are visually disturbing in practice. Thus, the estimated coefficients in Figure 3 are presented over an interval trimmed by 5% of the range of the observed daytime temperatures at each endpoint.

Acknowledgements

This research was funded by the National Institute for Global Environmental Change through the U.S. Department of Energy. We thank the numerous students and technicians involved in data collection and analysis at the flux tower sites. We also thank Toby N. Carlson (Pennsylvania State University) and Ming Xu (Rutgers University) for their comments and suggestions on a draft of this paper. Li's research was supported by a NSF Grant DMS0102505.

References

Ahl, D.E., S.T. Gower, D.S. Mackay, S.N. Burrows, J.M. Norman, and G. Diak, Light use efficiency of a heterogeneous forest in northern Wisconsin: Implications for remote

sensing and modeling net primary production, *Remote Sensing of Environment*, 2003. (In press)

Bakwin, P. S., P.P. Tans, D.F. Hurst, and C. Zhao, Measurements of carbon dioxide on very tall towers: Results of the NOAA/CMDL program, *Tellus*, 50b, 401-415, 1998.

Baldocchi, D.D., Measuring and modeling carbon dioxide and water vapor exchange over a temperate broad-leaved forest during the 1995 summer drought, *Plant, Cell and Environment, 20*, 1108-1122, 1997.

Baldocchi, D.D., J. Finnigan, K. Wilson, K.T. Paw U, and E. Falge, On measuring net ecosystem carbon exchange over tall vegetation on complex terrain, *Boundary-Layer Meteorology*, 96, 257-291, 2000.

Baldocchi, D. D., Falge, E, Gu, L., R. Olson, D. Hollinger, S. Running, P. Anthoni, Ch. Bernhofer, K. Davis, J. Fuentes, A. Goldstein, G. Katul, B. Law, X. Lee, Y. Malhi, T. Meyers, J.W. Munger, W. Oechel, K. Pilegaard, H.P. Schmid, R. Valentini, S. Verma, T. Vesala, K. Wilson and S. Wofsy, Fluxnet: a new tool to study the temporal and spatial variability of ecosystem-scale carbon dioxide, water vapor, and energy flux densities, *Bulletin of the American Meteorological Society 82*, 2415-2434, 2001.

Barford, C. C., S. C. Wofsy, M. L. Goulden, J. W. Munger, E. H. Pyle, S. P. Urbanski, L. Hutyra, S. R. Saleska, D. Fitzjarrald, K. Moore, Factors controlling long and short term sequestration of atmospheric CO_2 in a mid-latitude forest, *Science*, 294, 1688-1691, 2001.

Berger, B.W., K.J. Davis, C. Yi, P. S. Bakwin, and C. Zhao, Long-term carbon dioxide fluxes from a very tall tower in a northern forest: Flux measurement methodology, *J. Oceanic and Atmos. Tech.*, 18, 529-542, 2001.

Black, T.A, G. den Hartog, H.H. Neumann, P.D. Blanken, P.C. Yang, C. Russell, Z. Nesic, X. Lee, S.G. Chen, R. Staebler, and M.D. Novak, Annual cycles of water vapour and carbon dioxide fluxes in and above a boreal aspen forest, *Global Change Biology*, 2, 219-229, 1996.

Borken, W., Y.-J. Xu, R. Brumme, and N. Lamersdorf, A climate change scenario for carbon dioxide and dissolved organic carbon fluxes from a temperate forest soil: drought and rewetting effects, *Soil Sci. Soc. Am. J.*, 63, 1848-1855, 1999.

Budyko, M. I., *Climate and Life*, 508 pp., Academic Press, New York, 1974.

Cai, Z., J. Fan, and R. Li, Efficient estimation and inferences for varying-coefficient models, Journal of American Statistical Association, 95, 888-902, 2001.

Carey, E.V., R.M. Callaway and E.H. DeLucia, Increased photosynthesis offsets costs of allocation to sapwood in an arid environment, *Ecology*, 79, 2281-2291, 1998.

Chen, W.J., T.A. Black, P.C. Yang, A.G. Barr, H.H. Neumann, Z. Nesic, P.D. Blanken, M.D. Novak, J. Eley, R.J. Ketler, and A. Cuenca. Effects of climatic variability on the annual carbon sequestration by a boreal aspen forest, *Global Change Biology*, 5, 41-53, 1999.

Curtis, P.S. and X. Wang. A meta-analysis of elevated CO2 effects on woody plant mass, form, and physiology, *Oecologia*, 113, 299-313. 1998.

Curtis, P.S., C.S. Vogel, X. Wang, K.S. Pregitzer, D.R. Zak, J. Lussenhop, M. Kubiske, and J.A. Teeri, Gas exchange, leaf nitrogen, and growth efficiency of Populus tremuloides in a CO2 enriched atmosphere, *Ecological Applications*, 10, 3-17, 2000.

Davis, K. J., P. S. Bakwin, C. Yi, B. W. Berger, C. Zhao, R. Teclaw, and J. G. Isebrands, The annual cycles of CO2 and H2O exchange over a northern mixed forest as observed from a very tall tower, *Global Change Biology*, in press.

Ewers, B.E., D.S. Mackay, S.T. Gower, D.E. Ahl, S.N. Burrows, and S. Samanta, Tree species effects on stand transpiration in northern Wisconsin, Water resources research, 38, 10.1029/2001WR000830, 2002.

Falge, E., D. Baldocchi, R.J. Olson, P. Anthoni, M. Aubinet, C. Bernhofer, G. Burba, R. Ceulemans, R. Clement, H. Dolman, A. Granier, P. Gross, T. Grünwald, D. Hollinger, N.-O. Jensen, G. Katul, P. Keronen, A. Kowalski, C. Ta Lai, B. E. Law, T. Meyers, J. Moncrieff, E. Moors, J. W. Munger, K. Pilegaard, Ü. Rannik, C. Rebmann, A. Suyker, J. Tenhunen, K. Tu, S. Verma, T. Vesala, K. Wilson, S. Wofsy, Gap Filling Strategies for Defensible Annual Sums of Net Ecosystem Exchange, *Agricultural Forest and Meteorology*, 107, 43-69, 2001a.

Falge, E., D. Baldocchi, R.J. Olson, P. Anthoni, M. Aubinet, C. Bernhofer, G. Burba, R. Ceulemans, R. Clement, H. Dolman, A. Granier, P. Gross, T. Grünwald, D. Hollinger, N.-O. Jensen, G. Katul, P. Keronen, A. Kowalski, C. Ta Lai, B. E. Law, T. Meyers, J. Moncrieff, E. Moors, J. W. Munger, K. Pilegaard, Ü. Rannik, C. Rebmann, A. Suyker, J. Tenhunen, K. Tu, S. Verma, T. Vesala, K. Wilson, S. Wofsy, Gap Filling Strategies for Longterm Energy Flux Data Sets, *Agricultural Forest and Meteorology* 107, 71-77, 2001b.

Fan, J., I. Gijbels, *Local Polynomial Modelling and Its Applications*, pp. 341, Chapman & Hall, London, 1996.

Fan, J. and R. Li, Semiparametric Modeling for Longitudinal Data:Estimation, Variable Selection, Nonparametric Goodness-of-fit.Technical Report, 02-02, Department of Statistics, Pennsylvania State University, University Park, 2002.

Fan, J., C. Zhang, and J. Zhang, Generalized likelihood ratio statistics and Wilks phenomenon, The Annals of Statistics, 29, 153-193, 2001.

Farquhar, G.D., S. von Caemmerer, and J.A. Berry , A biochemical model of photosynthetic CO_2 assimilation in leaves of C3 species, *Planta*, 149, 78-90, 1980.

Farquhar G.D., and S. von Caemmerer, Modeling of photosynthetic response to environmental conditions, in *Encyclopedia of Plant Physiology*, New Series, Vol. 12B , edited by O.L. Lange, P.S. Nobel and C.B. Osmond, pp. 549-587, Springer-Verlag, Berlin, 1982.

Field, C., and H. A. Mooney, The photosynthesis-nitrogen relationship in wild plants, In: *On the Economy of Plant Form and Function* (T. J. Givnish, ed.), pp. 25-55, Cambridge University Press, Cambridge, 1986.

Field, C. B., Ecological scaling of carbon gain to stress and resource availability, In: *Response of Plants to Multiple Stresses* (Ed. By H. A. Mooney, W. E. Winner and E. J. Pell), pp. 35-65, Academic Press, San Diego, 1991.

Flanagan, L.B., L.A. Wever, P.J. Carlson, Seasonal and interannual variation in carbon dioxide exchange and carbon balance in a northern temperate grassland, *Global Change Biolog*, 8, 599-615, 2002.

Goetz, S.J. and S.D. Prince, Modeling terrestrial carbon exchange and storage: the evidence for and implications of functional convergence in light use efficiency, *Advances in Ecological Research*, 28, 57-92, 1999.

Goulden, M.L., J.W. Munger, S.M. Fan, B.C. Daube, and S.C. Wofsy, Measurements of carbon sequestration by long-term eddy covariance: Methods and a critical evaluation of accuracy, *Global Change Biology, 2*, 1996.

Goulden, M.L., B.C. Daube, S.M. Fan, D. J. Sutton, A. Bazzaz, J.W. Munger, and S.C. Wofsy, Physiological responses of a black spruce forest to weather, *J. Geophys. Res.,102*, 28987-28996, 1997.

Gower, S.T., C.J. Kucharik and J.M. Norman, Direct and indirect estimation of leaf area index, f_{apar}, and net primary production of terrestrial ecosystems, *Remote Sensing of Environment*, 70 , 29-51, 1999.

Gu, L., D.D. Baldocchi, S. B. Verma, T. A. Black, T. Vesala, E. M. Falge, P.R. Dowty, Superiority of diffuse radiation for terrestrial ecosystem productivity, *Journal of Geophysical Research 107*, 2002.

Gutschick, V. P., *A Functional Biology of Crop Plants*, Croom Helm, London. 230 pp., 1987.

Gutschick, V.P., C.J. Maxwell, M. Montes-Helu, F. Najera, E. Jackson, E. Mortenson, and A. Soto, Physiological control of carbon and water fluxes in the Chequamegon National Forest, its variability and consequences, *Global Change Biology*, submitted. 2002.

Hanan, N. P., G. Burba, S. B. Verma, J. A. Berry, A. Suyker, E. A. Walter-Shea, Inversion of net ecosystem CO_2 flux measurements for estimation of canopy PAR absorption, *Global Change Biology*, 8, 563-574, 2002.

Hart, J. D., Nonparametric Smoothing and Lack-of-fit Tests, pp. 287, Springer, New York, 1997.

Hollinger D.Y., F.M. Kelliher, J.N. Byers, J.E. Hunt, T.M. McSeveny, and P. L. Weir, Carbon dioxide exchange between an undisturbed old-growth temperate forest and the atmosphere, *Ecology*, 75, 134-150, 1994.

Hollinger D.Y., F.M. Kelliher, E.-D. Schulze, G. Bauer, A. Arneth, J.N. Byers, J.E. Hunt, T.M. McSeveny, K.I. Kobak, A. Sogachov, F. Tatarinov, A. Varlagin, W. Ziegler, N.N. Vygodskaya, Forest-atmosphere carbon dioxide exchange in eastern Siberia. *Agricultural and Forest Meteorology*, 90, 291-306, 1998.

Hungate, B.A., M. Reichstein, P. Dijkstra, D. Johnson, G. Hymus, J.D. Tenhunen, B.G. Drake, Evapotranspiration and soil water content in a scrub-oak woodland under carbon dioxide enrichment, *Global Change Biology*, 8, 289-298, 2002.

Hutchison, B.A. and D.D. Baldocchi, Forest Meteorology, In**:** *Analysis of Biogeochemical Cycling Processes in Walker Branch Watershed*, (Eds) D.W. Johnson and R.I. Van Hook. Springer-Verlag, pp. 21-95, 1989.

Hurwitz, M.D., D.M. Ricciuto, K.J. Davis, W. Wang, C. Yi, M.P. Butler and P.S. Bakwin, Advection of carbon dioxide in the presence of storm systems over a northern Wisconsin forest, *Journal of Atmospheric Science*, 2003. (In review)

Infante J.M., C. Damesin, S. Rambal & R., Fernandez-Alès, Modeling leaf gas exchange in holm-oak trees in southern Spain, *Agric. Forest Meteorol.*, 95, 203-223**:** 1999.

Jarvis, P.G., The interpretations of the variations in leaf water potential and stomatal conductance found in canopies in the field, *Phil. Trans. R. Soc*. B 273, 543-610, 1976.

Jarvis, P.G., and J. W. Leverenz, Productivity of temperate, deciduous and evergreen forests, In: *Physiological Plant Ecology IV. Ecosystem Processes: Mineral Cycling, Productivity and Man's Influence*, edited by O. L. Lange, P.S. Nobel, C.B. Osmond and H. Ziegler, New York, Springer-Verlag, 1983.

Jarvis, P.G., and K.G. McNaughton, Stomatal control of transpiration: Scaling up from leaf to region, *Adv. Ecol. Res*., 15, 1-49, 1986.

Jarvis, P. G., and A. P. Sandford, Temperate forests, In: *Photosynthesis in Contrasting Environments Topics in Photosynthesis Research*, Vol. 7 (N.R. Baker and S.P. Long eds.) Elsevier, Amsterdam, pp. 63-102, 1986.

Jarvis, P.G., J.M. Massheder, S.H. Hale, J.B. Moncrieff, M. Rayment, and S.L Scott, Seasonal variation of carbon dioxide, water vapor, and energy exchanges of a boreal Black Spruce forest, *Journal of Geophysical Research*, 102, 28953-28966, 1997.

Johnson, D.W., and R. I. van Hook (Eds.), *Analysis of Biogeochemical Cycling Processes in Walker Branch Watershed*, Springer-Verlag, New York, 1989.

Jurik, T. W., G. M. Briggs, and D. M. Gates, *Carbon Dynamics of Northern Hardwood Forest: Gas Exchange Characteristics*, DOE/EV/10091-1 TR019, NII Service, U. S. Dept. of Energy, Washington, D. C., 1985.

Kelly, R. D., E. R. Hunt, Jr., W. A. Reiners, W. K. Smith, J. M. Welker, Relationships between daytime carbon dioxide flux and absorbed photosynthetically active radiation for four different mountain/plains ecosystems, *Journal of Geophysical Research*, 107(D14): 19.1-19.8. As PDF: DOI 10.1029/2001JD001181.2002.

Lambers, H., F. S. Chapin III, and T. L. Pons, *Plant Physiological Ecology*, 540 pp., Springer-Verlag, New York, 1998.

Larcher, W., *Physiological Plant Ecology*, 302 pp., Springer-Verlag, New York, 1980.

Lee, R., *Forest Hydrology*, 349 pp., Columbia University Press, New York, 1980.

Li, R., N. Altman, and C. Yi, Nonlinear varying coefficient models and its applications, In preparation for *Journal of American Statistical Association*, 2003.

Lindroth, A., A. Grelle, and , A.-S. Morén, Long-term measurements of boreal forest carbon balance reveals large temperature sensitivity, *Global Change Biology*, 4, 443-450, 1998.

Long, S.P., Leaf Gas Exchange. In: *Photosynthetic Mechanisms and the Environment* (J. Baker and N.R. Baker, eds.) Elsevier, Amsterdam, pp.453-499, 1985.

Long, S.P., Modification of the response of photosynthetic productivity to rising temperature by atmospheric CO2 concentrations, Has its importance been underestimated? – Opinion, *Plant Cell and Environment*, 14, 729-739, 1991.

Luo, Y., S. Wan, D. Hui, and L. L. Wallace, Acclimatization of soil respiration to warming in a tall grass prairie, *Nature, 413*, 622-625, 2001.

Mackay, D.S., D.E. Ahl, B.E. Ewers, S.T. Gower, S.N. Burrows, S. Samanta, and K.J. Davis, Effects of aggregated classifications of forest composition on estimates of evapotranspiration in a northern Wisconsin forest, *Global Change Biology*, 8, 1-13, 2002.

Meidner, H. and T. A. Mansfield, *Physiology of Stomata*, McGraw-Hill, New York, 1968.

McCaughey, J. H., P.M. Lafleur, D.W. Joiner, P.A. Bartlett, A.M. Costello, D.E. Jelinski, and M.G. Ryan, Magnitudes and seasonal patterns of energy, water, and carbon exchanges at a boreal young jack pine forest in the BOREAS northern study area, *Journal of Geophysical Research*, 102, 28997-29007, 1997.

McCree, K.J., The action spectrum, absorptance and quantum yield of photosynthesis in crop plants, *Agricultural Meteorology*, 9, 191-216, 1972.

McCree, K.J., Equation for the rate of dark respiration of white clover as function of dry weight, photosynthesis rate and temperature, *Crop Science*, 14, 509-514, 1974.

Meyers, T. P., A comparison of summertime water and CO2 fluxes over rangeland for well watered and drought conditions, *Agricultural and Forest Meteorology*, 106, 205-214, 2001.

Monteith, J.L., Solar radiation and productivity in tropical ecosystems, *Journal of Applied Ecology*, 9, 747 766, 1972.

Monteith, J.L., Climate and the efficiency of crop production in Britain, *Philosophical Transactions of the Royal Society of London*, B, 281, 277-294, 1977.

Moren, A.-S., A. Lindroth and A. Grelle, Water-use efficiency as a means of modeling net assimilation in boreal forests, Tree, 15, 67-74, 2001.

Moren, A-S., A. Lindroth, J.G.K. Flower-Ellis, E. Cienciala, and M. Mölder, Branch transpiration of a boreal forest scaled to tree and canopy using needle biomass distributions, Trees, 14, 384-397, 2000.

Nemani, R.R. and S.W. Running, Estimation of regional surface resistance to evapotranspiration from NDVI and thermal infrared AVHRR data, *Journal of Applied Meteorology*, 28, 276-284, 1989.

Pallardy, S. G., and T. T. Kozlowski, Water relations of Populus clones, *Ecology*, 57, 367-373, 1981.

Pilegaard, K., P. Hummelshoej, N.O. Jensen, Z. Chen, Two years of continuous CO_2 eddy-flux measurements over a Danish beech forest, *Agricultural and Forest Meteorology*,107, 29-41, 2001.

Price, D.T. and T.A.Black, Effects of short-term variation in weather on diurnal canopy CO2 flux and evapotranspiration of a juvenile Douglas-fir stand, *Agricultural and Forest Meteorology*, 50, 139-158, 1990.

Prince, S.D., A model of regional primary production for use with caose-resolution satellite data, *International Journal of Remote Sensing*, 12, 1313-1330, 1991.

Regehr, D. L., F. A. Bazzaz, and W. R. Bogges, Photosynthesis, transpiration and leaf conductance of Populus deltotdes in relation to flooding and drought, *Photosynthetica*, 9, 52-61, 1975.

Reichstein, M., J.D. Tenhunen, O. Roupsard, J.-M. Ourcival, S. Rambal, F. Miglietta, A. Peressotti, M. Pecchiari, G. Tirone, R Valentini, Severe drought effects on ecosystem CO_2 and H_2O fluxes in three Mediterranean evergreen ecosystems: revision of current hypotheses? *Global Change Biology*, 8, 999-1017, 2002.

Ruimy, A., P.G. Jarvis, D.D. Baldocchi and B.Saugier, CO2 fluxes over plant canopies: a literature review, *Advances in Ecological Research, 26*, 1-68, 1995.

Ruimy A., L. Kergoat, C. Field and B. Saugier, The use of CO2 flux measurements in the models of the global terrestrial carbon budget, *Global Change Biology*, **2**, 287-296, 1996.

Ruimy, A., L. Kergoat, A. Bondeau, ThE. Participants OF. ThE. Potsdam NpP. Model Intercomparison, Comparing global models of terrestrial net primary productivity (NPP): analysis of differences in light absorption and light-use efficiency, *Global Change Biology*, 5, 56-64, 1999.

Sala, A. and J.D. Tenhunen, Site-specific water relations and stomatal response of Quercus ilex L. in a Mediterranean watershed, *Tree Physiology*, 14, 601-617, 1994.

Sala, A. and J.D. Tenhunen, Simulations of canopy net photosynthesis and transpiration in Quercus ilex L. under the influence of seasonal drought. *Agric. and For. Meteorol*., 78, 203-222, 1996.

Schmid, H. P., C. S. B. Grimmond, F. Cropley, B. Offerele, and H.-B. Su, Measurements of CO2 and Energy Fluxes over a Mixed Hardwood Forest in the Midwestern United States, *Agricultural and Forest Meteorology*, 103, 355-373, 2000,.

Schulze, E.-D. and A.E. Hall, Stomatal responses, water loss, and CO2 assimilation rates of plants in contrasting environments, In: *Encyclopedia of Plant Physiology* (Eds O.L. Lange, P.S. Nobel, C.B. Osmond, and H. Ziegler), Vol. 12B, new series, Springer-Verlag, Berlin,181-230, 1982.

Suyker, A. E., S. B. Verma, Year-round observations of the net ecosystem exchange of carbon dioxide in a native tallgrass prairie, *Global Change Biology*, 7, 279-289, 2001.

Wand, M. P. and M.C. Jones, *Kernel Smoothing*, pp.212, Chapman & Hall, London, 1995.

Wilson, K.B., D.D. Baldocchi, Seasonal and interannual variability of energy fluxes over a broadleaved temperate deciduous forest in North America, *Agric. For. Meteorol.*,100, 1-18, 2000.

Wilson, K.B. and D.D. Baldocchi, Comparing independent estimates of carbon dioxide exchange over five years at a deciduous forest in the southern United States, *Journal of Geophysical Research*, 106, 34167, 2001.

Wofsy, S.C., M.L. Goulden, J.W. Munger, S.M. Fan, P.S. Bakwin, B.C. Daube, S.L. Bassow , and F.A. Bazzaz, Net exchange of CO2 in a mid-latitude forest, *Science, 260*, 1314-1317, 1993.

Yi, C., K. J. Davis, P. S. Bakwin, B. W. Berger, and L. Marr, The influence of advection on measurements of the net ecosystem-atmosphere exchange of CO_2 from a very tall tower, *Journal of Geophysical Research, 105*, 9991-9999, 2000.

Yi, C., K. J. Davis, B. W. Berger, P. S. Bakwin, Long-term observations of the dynamics of the continental planetary boundary layer, *Journal of the Atmospheric Science*, 58, 1288-1299, 2001.

Yi, C., K. J. Davis, P. S. Bakwin, T. Zhou, D. D. Baldocchi, A. L. Dunn, J. W. Munger, K. Wilson and S. C. Wofsy, The observed responses of forest carbon exchange to climate variations from daily to annual time scale in Northern America, to be submitted: *Journal of Geophysical Research*, 2003a.

Yi**, C.**, K. J. Davis, P. S. Bakwin, A.S. Denning, N. Zhang, J. Ch.-H. Lin, C. Gerbig, and S. C. Wofsy, The observed covariance between ecosystem carbon exchange and atmospheric boundary layer dynamics in North Wisconsin, to be submitted: *Journal of Geophysical Research*, 2003b.

Yu, G.-R., K. Nakayama, H. Matsumura, Comparison on variability of stomatal conductance between adaxial and abaxial surface of maize leaf, *J. Agric. Meteorology*, 52, 141-148, 1996.

Yu, G.-R., J. Zhuang, and Z-L. Yu, An attempt to establish a synthetic model of photosynthesis-transpiration based on stomatal behavior for maize and soybean plants grown in field, *Journal of Plant Physiology* , 158, 861-874, 2001.

Zine El Abidine, A., J.D. Stewart, P.Y. Bernier & A.P. Plamondon, Diurnal and seasonal variations in gas exchanges and water relations of two lowland and two upland black spruce ecotypes, *Canadian Journal of Botany*, 73, 716-722, 1995.

List of Illustrations

Figure 1. Agreement between the model calculated and measured F and comparison between the constant coefficient model (first column) and varying coefficient model (second column) calculations. All data used were daytime data in growing season (June through August) for the years 1995-1998 for WB; 1992-1999 for HV; 1997-1999 for WL and 1996-1997 for LW. The data in 1998 for LW was excluded because we could not obtain convergent result if it is included.

Figure 2. Contours of measured net uptake of CO_2 F in the space of T and Q in growing seasons. The data used were same as in Figure 1, and were processed by the statistical method described in A.1. The negative values on the lines indicate the net fixation of carbon by the ecosystem.

Figure 3. Relationships between light response parameters and temperature: (a) ecosystem respiration R; (b) ecosystem light-saturated net photosynthetic rate $F_{¥}$; (c) ecosystem apparent quantum yield α and (d) probability density of occurrence of temperature. The data used were the same as in Figure 1. 5% of each curve in (a)-(c) at the ends of low and high temperature were trimmed to reduce the uncertainties associated with the statistical boundary effects.

Figure 4. Observed diurnal patterns at WB for the relationship between: (a) F and T; (b) F and VPD; (c) F and Q; (d) F and R_n; (f) E and VPD; and (g) E and F. Each point (plus or circle) was the quasi-ensemble average for the half hourly data at the same time of day in the growing season in four years (1995-1998). The daytime began at 06:00 LST and ended at 20:00 LST (see Figure 6 for details), pluses denote the hours in the morning and circles denote the hours in the afternoon. The red curve represents data only in drier year 1995, and the blue curve represents data for the wetter year 1998. The dotted lines in the color curves denote morning and solid ones for afternoon.

Figure 5. Same as Figure 4, but for the grassland ecosystem LW. The plus/circle curves included growing data of 1996, 1997 and 1998. Red one was only for driest year 1998 and blue one for wettest year 1996.

Figure 6. Assimilation rate (A) versus evapotranspiration (E) at WB. The data have been averaged in half-hour bins by local standard time. Subscripts am and pm denote morning and afternoon constrained by equal E.

Figure 7. Diurnal distributions of the equivalent canopy conductance and difference between the mean canopy intercellular and ambient CO_2 concentrations. The subscripts am and pm indicate morning and afternoon respectively as defined in Figure 6.

Figure 8. Relationships between the equivalent canopy conductance g, mean canopy intercellular CO_2 concentrations C_i, ambient CO_2 concentrations C_a, and assimilation rates A. The supply functions are indicated by dashed lines, the slopes of which give the equivalent canopy conductance. The curved line is the demand function. Subscripts am and pm denote morning and afternoon as defined in Figure 6. {This figure is not very well explained in the text.}

Figure 9. Relationships between: (a) the ecosystem WUE and temperature and (b) *VPD* and temperature. The hours in the morning are indicated by pluses and the hours in afternoon by circles. The data used were the same as in Figure 1.

Figure 10. The photosynthetic capacity F_m versus dryness across the four sites. F_m was defined as the average value of the net uptake of CO_2 measured between 11:30 and 12:30 local standard time in the growing season of each year at each site. The dryness was defined in (10). F_m in 1996 at LW site (LW96) was omitted in the plot due a lack of data to compute dryness for that year.

Table 1. Generalized Likelihood Ratio Tests

Site	WB	HV	WL	LW
r_KGLRT	920.1703	394.1782	135.5925	310.6652
Approximate d.f.	10	13	9	12
P-value	<0.0001	<0.0001	<0.0001	<0.0001

Table 2. Data for annual net radiation $\overline{R}_n$, annual precipitation $\overline{P}$, *Dryness* and the photosynthetic capacity F_m that was mean F at noon over the growing season.

Site-year code	$\overline{R}_n$ (MJ m^{-2} yr^{-1})	$\overline{P}$ (mm yr^{-1})	*Dryness*	F_m (*m*mol m^{-2} s^{-1})
WB95	3106	1253	0.992	-14.54
WB96	3080	1705	0.723	-21.33
WB97	3066	1450	0.846	-19.79
WB98	2707	1663	0.651	-18.93
HV92	2117	1102	0.769	-13.06
HV93	2194	1227	0.716	-16.58
HV94	2024	1326	0.611	-15.95
HV95	2560	1077	0.950	-16.67
HV96	2346	1470	0.639	-16.61
HV97	2470	933	1.059	-17.41
HV98	2286	955	0.958	-13.87
HV99	2943	1027	1.146	-16.92
WL97	2458	1092	0.901	-10.56
WL98	2406	526	1.830	-7.31
WL99	2090	706	1.184	-7.57
LW97	3279	938	1.398	-8.27
LW98	3228	715	1.807	2.74

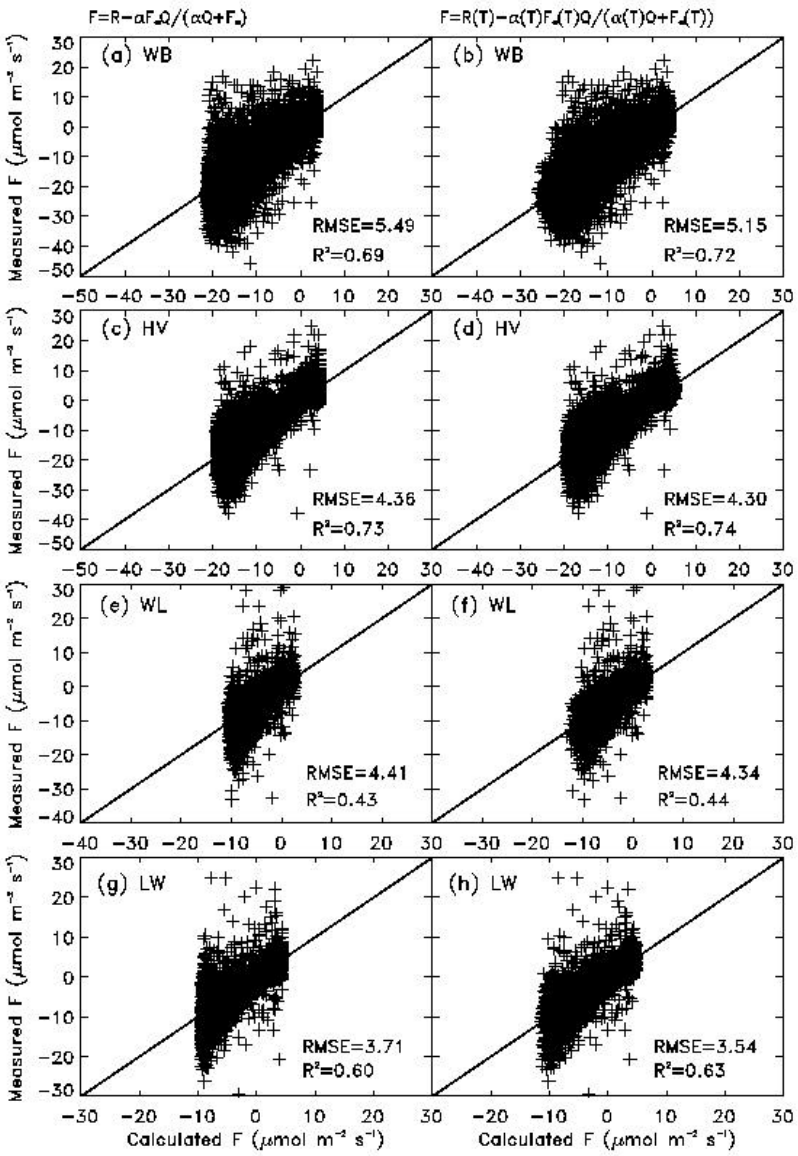

Figure 1 Agreement between the model calculated and measured *F* and comparison between the constant coefficient model (first column) and varying coefficient model (second column) calculations. All data used were daytime data in growing season (June through August) for the years 1995-1998 for WB; 1992-1999 for HV; 1997-1999 for WL and 1996-1997 for LW. The data in 1998 for LW was excluded because we could not obtain convergent result if it is included.

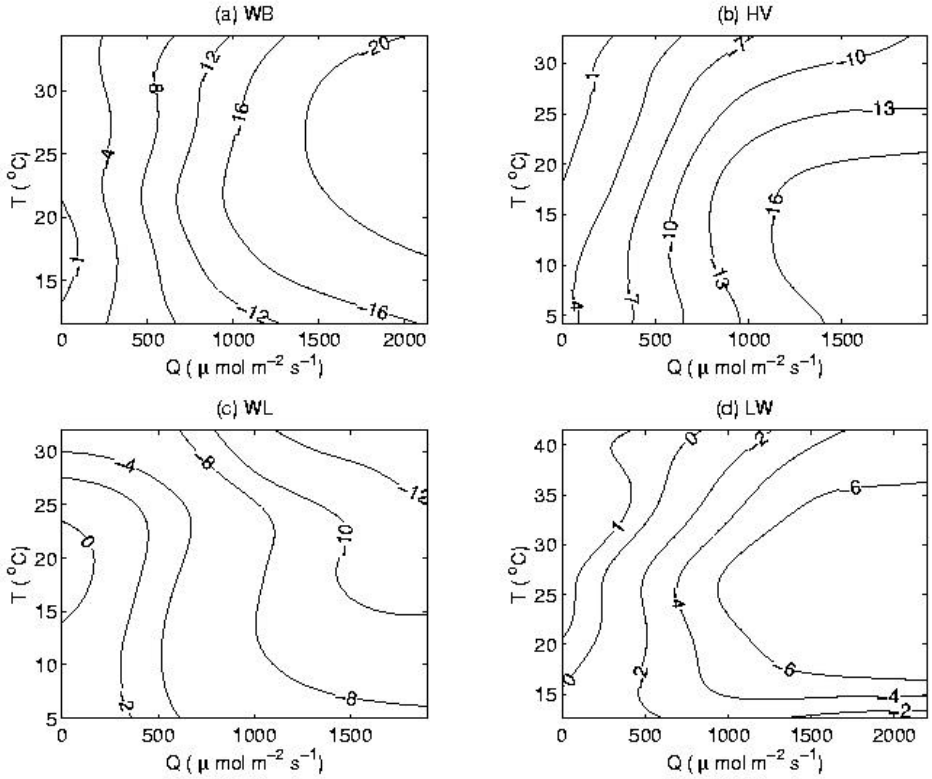

Figure 2 Contours of measured net uptake of CO_2 F in the space of T and Q in growing seasons. The data used were same as in Figure 1, and were processed by the statistical method described in A.1. The negative values on the lines indicate the net fixation of carbon by the ecosystem.

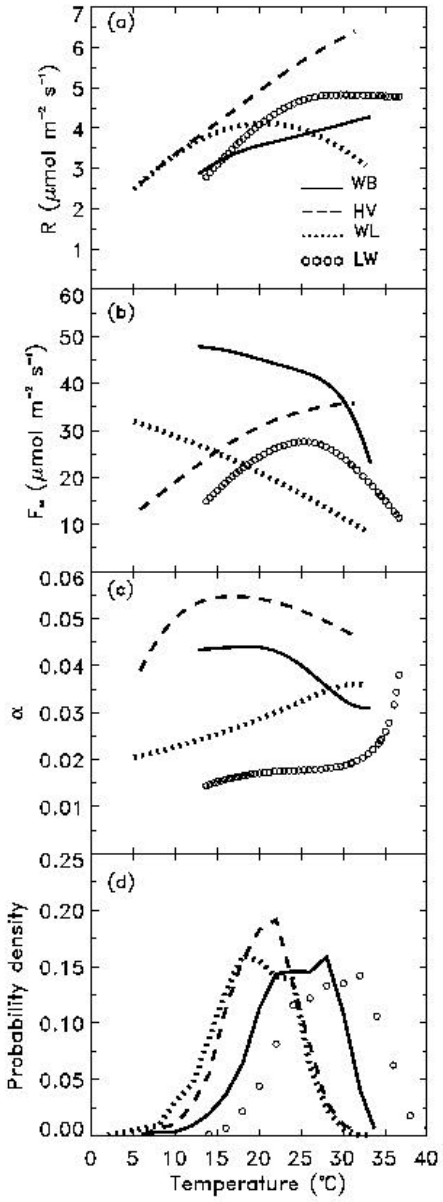

Figure 3 Relationships between light response parameters and temperature: (a) ecosystem respiration *R*; (b) ecosystem light-saturated net photosynthetic rate $F_{¥}$; (c) ecosystem apparent quantum yield α and (d) probability density of occurrence of temperature. The data used were the same as in Figure 1. 5% of each curve in (a)-(c) at the ends of low and high temperature were trimmed to reduce the uncertainties associated with the statistical boundary effects.

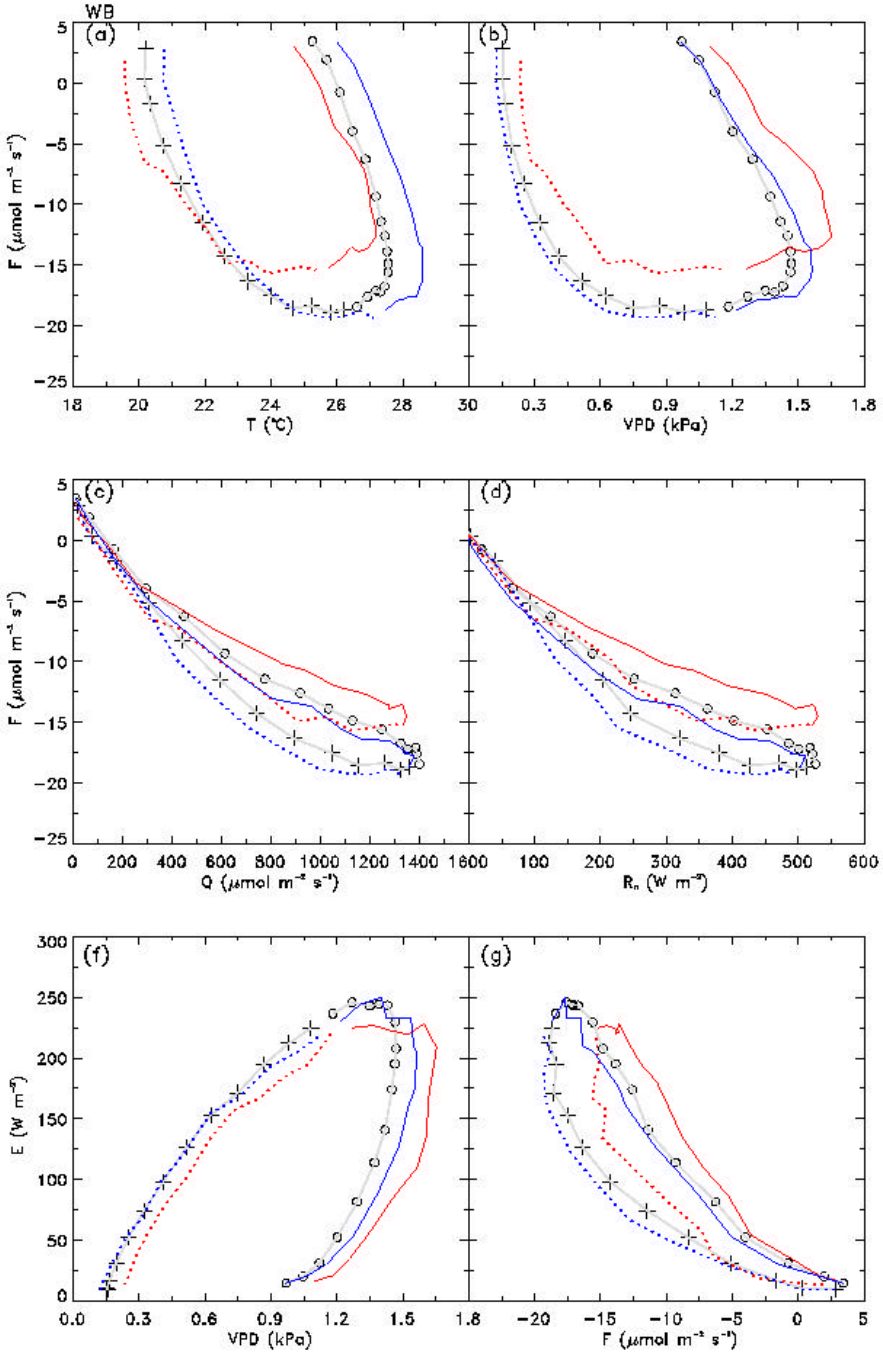

Figure 4 Observed diurnal patterns at WB for the relationship between: (a) *F* and *T*; (b) *F* and *VPD*; (c) *F* and *Q*; (d) *F* and R_n; (f) *E* and *VPD*; and (g) *E* and *F*. Each point (plus or circle) was the quasi-ensemble average for the half hourly data at the same time of day in the growing season in four years (1995-1998). The daytime began at 06:00 LST and ended at 20:00 LST (see Figure 6 for details), pluses denote the hours in the morning and circles denote the hours in the afternoon. The red curve represents data only in drier year 1995, and the blue curve represents data for the wetter year 1998. The dotted lines in the color curves denote morning and solid ones for afternoon.

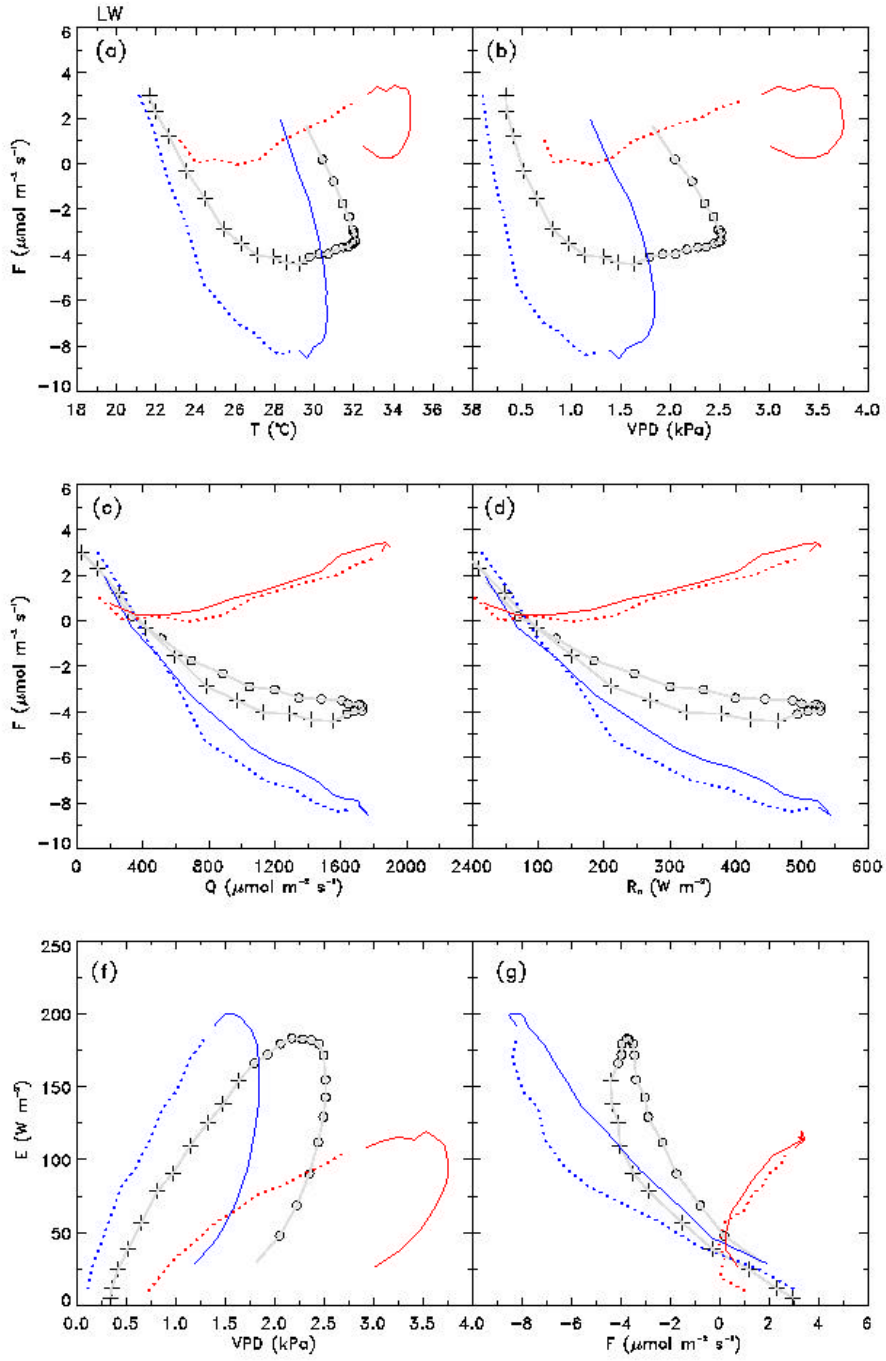

Figure 5 Same as Figure 4, but for the grassland ecosystem LW. The plus/circle curves included growing data of 1996, 1997 and 1998. Red one was only for driest year 1998 and blue one for wettest year 1996.

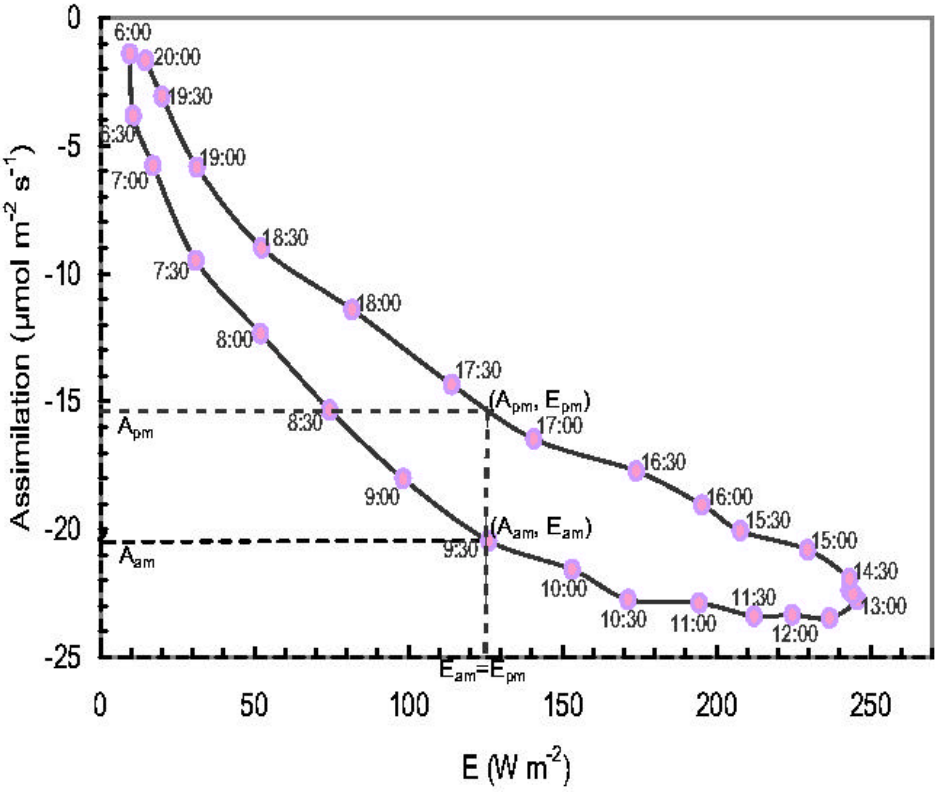

Figure 6 Assimilation rate (*A*) versus evapotranspiration (*E*) at WB. The data have been averaged in half-hour bins by local standard time. Subscripts am and pm denote morning and afternoon constrained by equal *E*.

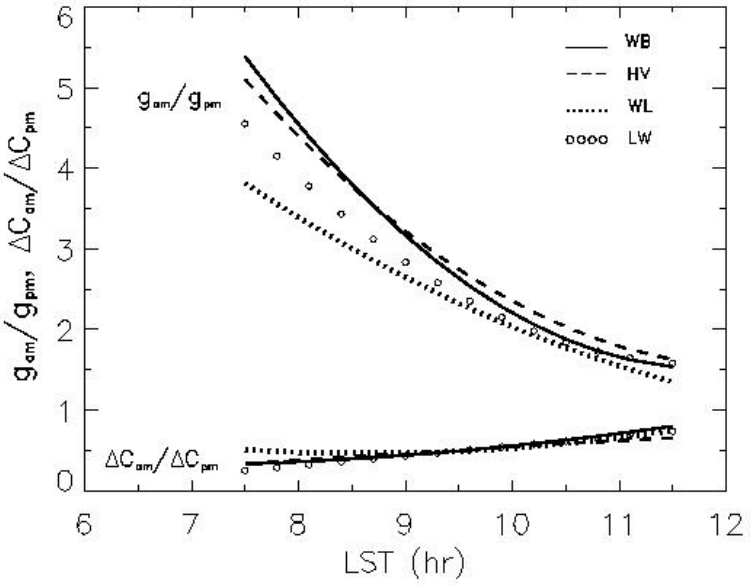

Figure 7 Diurnal distributions of the equivalent canopy conductance and difference between the mean canopy intercellular and ambient CO_2 concentrations. The subscripts am and pm indicate morning and afternoon respectively as defined in Figure 6.

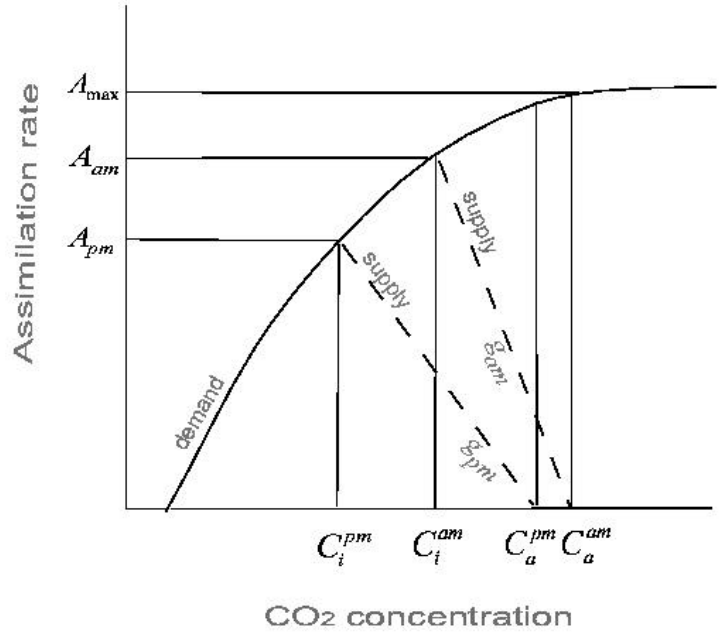

Figure 8 Relationships between the equivalent canopy conductance *g*, mean canopy intercellular CO_2 concentrations C_i, ambient CO_2 concentrations C_a, and assimilation rates *A*. The supply functions are indicated by dashed lines, the slopes of which give the equivalent canopy conductance. The curved line is the demand function. Subscripts am and pm denote morning and afternoon as defined in Figure 6.

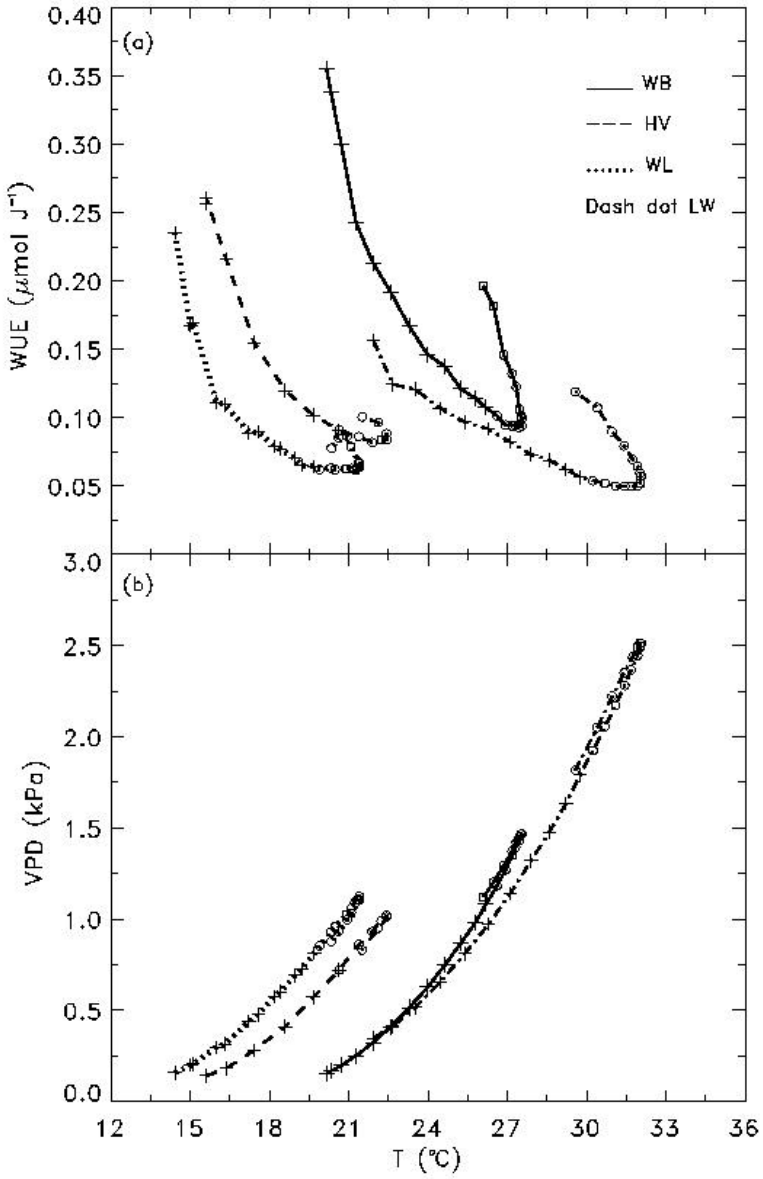

Figure 9 Relationships between: (a) the ecosystem WUE and temperature and (b) *VPD* and temperature. The hours in the morning are indicated by pluses and the hours in afternoon by circles. The data used were the same as in Figure 1.

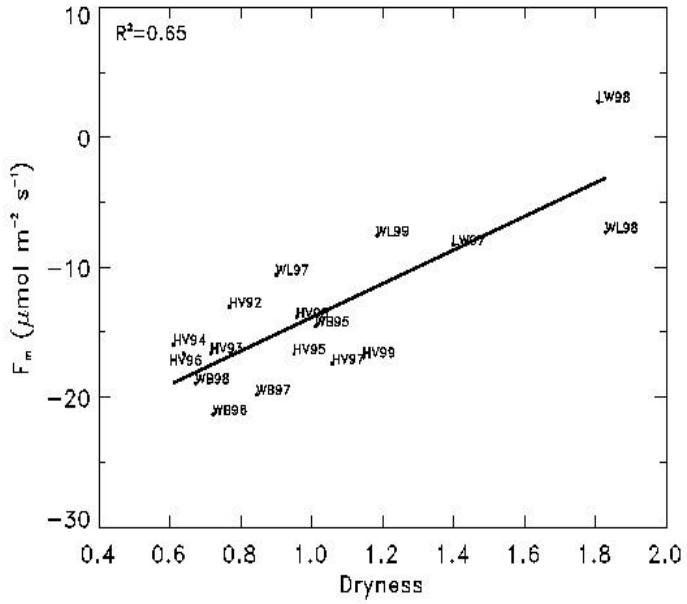

Figure 10 The photosynthetic capacity F_m versus dryness across the four sites. F_m was defined as the average value of the net uptake of CO_2 measured between 11:30 and 12:30 local standard time in the growing season of each year at each site. The dryness was defined in (10). F_m in 1996 at LW site (LW96) was omitted in the plot due a lack of data to compute dryness for that year.